

## Theory and simulations of electrostatic field error transport

Daniel H. E. Dubin

*Department of Physics, University of California at San Diego, La Jolla, California 92093, USA*

(Received 28 April 2008; accepted 2 May 2008; published online 16 July 2008)

Asymmetries in applied electromagnetic fields cause plasma loss (or compression) in stellarators, tokamaks, and non-neutral plasmas. Here, this transport is studied using idealized simulations that follow guiding centers in given fields, neglecting collective effects on the plasma evolution, but including collisions at rate  $\nu$ . For simplicity the magnetic field is assumed to be uniform; transport is due to asymmetries in applied electrostatic fields. Also, the Fokker–Planck equation describing the particle distribution is solved, and the predicted transport is found to agree with the simulations. Banana, plateau, and fluid regimes are identified and observed in the simulations. When separate trapped particle populations are created by application of an axisymmetric squeeze potential, enhanced transport regimes are observed, scaling as  $\sqrt{\nu}$  when  $\nu < \omega_0 < \omega_B$  and as  $1/\nu$  when  $\omega_0 < \nu < \omega_B$  (where  $\omega_0$  and  $\omega_B$  are the rotation and axial bounce frequencies, respectively). These regimes are similar to those predicted for neoclassical transport in stellarators. © 2008 American Institute of Physics. [DOI: 10.1063/1.2936874]

### I. INTRODUCTION

Irreversible processes driven by the interaction of a plasma with static electric and/or magnetic fields are of central importance in plasma theory and experiment. For example, in the theory of neoclassical transport, a magnetically confined plasma interacts with static electric and/or magnetic field asymmetries, causing irreversible flows of particles, momentum, and energy across the magnetic field.<sup>1–4</sup> In storage rings and accelerators, charged particle beams interact with static electric and magnetic field asymmetries in the accelerator or ring structure, resulting in beam degradation.<sup>5–7</sup> In rf heating and current drive, an applied wave heats and accelerates the plasma particles.<sup>8–11</sup> When viewed in the wave frame, the induced current and heating can also be thought of as irreversible processes driven by interaction between a moving plasma and a static field asymmetry.

Even linear and nonlinear Landau damping can be thought of as an interaction between a moving plasma and a static field asymmetry when viewed in the wave frame. While these two processes are not necessarily irreversible, damping rates can still be determined using transport theory by equating the Joule heating power to the wave energy loss rate,<sup>12,13</sup> with the regime of linear Landau damping equivalent to the plateau regime in neoclassical transport, and the regime of nonlinear Landau damping equivalent to the banana regime.

Over the decades, each of these subjects has spawned innumerable papers. Theory in each area is well developed, and simulations have tested almost every aspect of the theory. There have also been detailed experimental studies in many cases (Landau damping,<sup>14,15</sup> rf heating, and current drive,<sup>6,7</sup> for example). But in other cases (in particular, neoclassical transport), experiments have never adequately tested the theory. In neutral plasma experiments, early work on quiescent discharges was broadly consistent with theory;<sup>16</sup> but in many experiments neoclassical transport is

masked by anomalous transport caused by nonlinear saturation of collective plasma instabilities. In non-neutral plasma experiments, where such instabilities are absent, detailed measurements of transport over the course of several decades have still failed to make close contact with neoclassical theory.<sup>17–20</sup> Interpretation of experimental results is often complicated by the interplay of multiple effects, even in the simplest experimental design.

In order to make progress, it is this author's view that further simplification is necessary. This paper describes numerical simulation and accompanying theory of neoclassical transport in a set of three different experimental geometries, of increasing complexity. In each case, particle mobility and/or diffusion across the magnetic field is measured and compared to theoretical predictions. Energy and momentum transport caused by field errors is also analyzed. In order to simplify the theory, we consider only transport driven by electrostatic asymmetries, taking the magnetic field to be uniform. Also, the potentials acting on the plasma are assumed to be time-independent; self-consistent potentials arising from the plasma evolution are simply ignored. Use of prescribed potentials has the advantage of considerably simplifying the simulations, and removing certain difficult to analyze nonlinear effects from the theory.

Even with these simplifications, the simulations and theory uncover a wealth of physics, much of which can be connected to the “classic” neoclassical results obtained decades ago for plasmas trapped in toroidal magnetic fields. One minor complication is that here equilibrium plasma rotation due to  $\mathbf{E} \times \mathbf{B}$  drifts is included in the analysis, and transport coefficients that depend on  $\mathbf{E} \times \mathbf{B}$  rotation frequency  $\omega_0$  are derived. (This dependence was also considered in earlier work on transport in tokamaks<sup>21</sup> and magnetic mirrors.<sup>22</sup>)

When the plasma equilibrium is assumed to be a long uniform column oriented along the direction of the magnetic field  $\mathbf{B} = B_0 \hat{z}$ , and an electrostatic asymmetry of the form

$\delta\phi(r, \theta, z) = \varepsilon(r) \cos(\ell\theta + kz)$  is applied (where  $\varepsilon/T \ll 1$  is assumed), the resulting radial transport displays the expected neoclassical behavior, breaking into banana, plateau, and fluid regimes depending on the collision frequency  $\nu$ <sup>1</sup>.

For large collision frequencies,  $\nu > k\bar{v}$ , where  $\bar{v}$  is the thermal speed, an analysis based on fluid equations provides the transport coefficients. In this fluid regime, radial particle transport is primarily caused by dissipation associated with compression and expansion of the plasma as it rotates through the field error. Temperature and velocity gradients can also lead to irreversible fluxes of particles, energy and momentum as the field error transports particles across the magnetic field.

For small collision frequencies,  $\nu < (\varepsilon/T)^{3/2} k\bar{v}$ , transport coefficients are linear functions of  $\nu$ .<sup>23,24</sup> The scaling of the radial diffusion coefficient  $D_r$  in this ‘‘banana regime’’ may be understood from the following argument. Particles become trapped in the field asymmetry when they have an axial velocity  $v_z$  that satisfies

$$\frac{m}{2}(v_z - \ell\omega_0/k)^2 < \varepsilon. \quad (1)$$

Such trapped particles execute axial oscillations in the field error at roughly the trapping frequency  $\omega_T = \sqrt{k^2\varepsilon/m}$ . In these oscillations, the particles also drift radially, with a radial ‘‘banana orbit’’ width  $\Delta r$  of order  $\ell\sqrt{2\varepsilon/m}/kr\Omega_c$ , where  $\Omega_c = eB/mc$  is the cyclotron frequency. This estimate follows from the product of the radial drift velocity  $\ell c\varepsilon/eBr$  and the period  $\omega_T^{-1}$  of the oscillation. Transport occurs as particles become collisionally detrapped and then retrapped.

The size of the step in this process is  $\Delta r$ . The time between steps is the time  $\Delta t$  required to be detrapped from the banana orbit, of order  $\varepsilon/(\nu T)$  (the time needed to diffuse in energy by order  $\varepsilon$ ). The radial particle diffusion coefficient  $D_r$  is therefore roughly

$$D_r \sim f \frac{\Delta r^2}{\Delta t}, \quad (2)$$

where  $f$  is the fraction of particles that take part in the banana orbits, of order  $f \sim e^{-\ell^2\omega_0^2/2k^2\bar{v}^2} \sqrt{\varepsilon/T}$  for a Maxwellian distribution. Putting these estimates together yields

$$D_r \sim \nu \sqrt{\frac{\varepsilon}{T}} \frac{\ell^2\bar{v}^2}{k^2 r^2 \Omega_c^2} e^{-\ell^2\omega_0^2/2k^2\bar{v}^2} \quad (3)$$

in the banana regime. This banana regime estimate is sensible only when the particles are able to execute a full trapping oscillation before they are collisionally detrapped. This requires  $\omega_T \Delta t \gtrsim 1$ , which implies

$$(\varepsilon/T)^{3/2} k\bar{v} > \nu \quad (4)$$

for the banana regime.

For  $k\bar{v}(\varepsilon/T)^{3/2} < \nu < k\bar{v}$ , the transport is in the plateau regime. Trapped particles no longer complete an entire banana orbit, so the size of the radial step is reduced to  $\Delta r \omega_T \Delta t$ . The diffusion coefficient is now given by

$$D_r \sim f_\nu \frac{(\Delta r \omega_T \Delta t)^2}{\Delta t}, \quad (5)$$

where  $f_\nu$  is the fraction of particles in resonance with the error,

$$f_\nu \sim e^{-\ell^2\omega_0^2/2k^2\bar{v}^2}/(k\bar{v}\Delta t). \quad (6)$$

This estimate yields the plateau regime diffusion coefficient

$$D_r \sim \left(\frac{\varepsilon}{T}\right)^2 \frac{\ell^2\bar{v}^3}{kr^2\Omega_c^2} e^{-\ell^2\omega_0^2/2k^2\bar{v}^2}. \quad (7)$$

The previous descriptions of banana, plateau and fluid regime transport were based on an equilibrium plasma with periodic boundary conditions along  $\mathbf{B}$ . For a plasma of finite length, we find that the same three regimes can occur.

However, if the plasma equilibrium has even small fractions of particles that are trapped in localized potential wells within the plasma column, these equilibrium trapped particles can have a large effect on the transport. The field asymmetry affects these particles differently than untrapped particles, leading to strong gradients in the velocity distribution near the separatrix between trapped and untrapped particles, which produce enhanced transport. Two regimes are identified, a  $\sqrt{\nu}$  and a  $1/\nu$  regime, depending on the ratios of the rotation, collision, and axial bounce frequencies. Both regimes have also been discussed in work on neoclassical transport in stellarators,<sup>2</sup> and  $\sqrt{\nu}$  transport has been related to the damping of trapped particle modes in tokamaks<sup>25</sup> and non-neutral plasmas.<sup>26</sup> Scaling of the transport in these regimes is discussed in Sec. IV C.

In Sec. II, the general theory of transport due to electrostatic asymmetries imposed on a cylindrical magnetically confined plasma equilibrium is developed from first principles. This theory recapitulates much of the earlier work on transport in more complicated toroidal geometries. In Sec. III, the particle simulation methods employed here are described. In Sec. IV, three examples of transport are analyzed and compared to the simulations.

## II. TRANSPORT THEORY

In this section the general theory of transport due to an electrostatic field error is developed. The magnetic field is assumed to be uniform,  $\mathbf{B} = B\hat{z}$ , and sufficiently large so that the guiding-center approximation is valid. In this approximation, cyclotron motion is neglected and particle dynamics are described by the guiding-center equations,

$$\frac{d\theta}{dt} = \frac{\partial\phi}{\partial p_\theta}, \quad \frac{dp_\theta}{dt} = -\frac{\partial\phi}{\partial\theta}, \quad (8)$$

$$\frac{dz}{dt} = v_z, \quad \frac{dp_z}{dt} = -\frac{\partial\phi}{\partial z},$$

where  $(r, \theta, z)$  are cylindrical coordinates,  $p_\theta$  is the canonically conjugate momentum to  $\theta$  given by

$$p_\theta = \frac{eB}{2c} r^2, \quad (9)$$

$p_z = mv_z$  is the linear momentum conjugate to  $z$ , and  $\phi(p_\theta, \theta, z)$  is the electrostatic potential energy of a plasma charge  $e$ , written for convenience in terms of  $p_\theta$  rather than  $r$  via Eq. (9). (Note that  $\phi$  is the true energy measured in ergs, not statvolts.) Equations (8) are of Hamiltonian form with energy

$$H = \frac{p_z^2}{2m} + \phi(p_\theta, \theta, z) \quad (10)$$

a constant of the motion (in the absence of collisions and time dependence in  $\phi$ ).

When collisions are included, a collection of particles described by the distribution function  $f(\theta, p_\theta, z, p_z, t)$  will evolve according to

$$\frac{\partial f}{\partial t} + [f, H] = \hat{C}f, \quad (11)$$

where  $[ ]$  is a Poisson bracket defined by

$$[f, g] = \frac{\partial f}{\partial \theta} \frac{\partial g}{\partial p_\theta} - \frac{\partial f}{\partial p_\theta} \frac{\partial g}{\partial \theta} + \frac{\partial f}{\partial z} \frac{\partial g}{\partial p_z} - \frac{\partial f}{\partial p_z} \frac{\partial g}{\partial z}, \quad (12)$$

and  $\hat{C}$  is the collision operator.

Various forms of the collision operator have been used in solving Eq. (11). In much of what follows, we assume that the operator has the following properties:

$$\int dp_z \hat{C}f = \int dp_z p_z \hat{C}f = \int dp_z H \hat{C}f = 0. \quad (13)$$

That is, the operator conserves particle number, momentum, and energy. (Later, in Sec. II H we will modify the theory to allow for operators that do not satisfy the latter two requirements.) Also, we require that  $\hat{C}$  is invariant under time reversal, i.e., ( $p_z \rightarrow -p_z, B \rightarrow -B$ ).

## A. Fluid equations

By taking velocity moments of Eq. (11), fluid equations for density, axial velocity, and energy can be obtained. We will integrate these fluid variables over  $\theta$  and  $z$  since the integrated functions enter the transport theory and simulations. The  $\theta$ - and  $z$ -integrated density is defined as

$$\bar{n}(p_\theta, t) \equiv \int d\theta dz dp_z f, \quad (14)$$

the mean axial velocity is

$$\bar{V}(p_\theta, t) \equiv (m\bar{n})^{-1} \int d\theta dz dp_z p_z f, \quad (15)$$

and the mean energy per particle,

$$\bar{E}(p_\theta, t) \equiv \bar{n}^{-1} \int d\theta dz dp_z H f. \quad (16)$$

The mean energy  $\bar{E}$  can also be written as  $\bar{E} = \bar{E}' + m\bar{V}^2/2$ , where

$$\bar{E}' = \bar{T}/2 + \bar{\phi} \quad (17)$$

is the mean energy as seen in a frame moving with velocity  $\bar{V}$ ,  $\bar{T}$  is the plasma temperature given by

$$\bar{T}(p_\theta, t) = (m\bar{n})^{-1} \int d\theta dz dp_z (p_z - m\bar{V})^2 f, \quad (18)$$

and  $\bar{\phi}$  is the  $\theta$  and  $z$ -averaged potential,

$$\bar{\phi}(p_\theta, t) = \bar{n}^{-1} \int d\theta dz dp_z \phi f. \quad (19)$$

The fluid equations for these variables are

$$\frac{\partial \bar{n}}{\partial t} + \frac{\partial}{\partial p_\theta} \Gamma_{\bar{n}} = 0, \quad (20)$$

$$m\bar{n} \frac{\partial \bar{V}}{\partial t} + \frac{\partial \Gamma'_{\bar{V}}}{\partial p_\theta} + m\Gamma_{\bar{n}} \frac{\partial \bar{V}}{\partial p_\theta} - F_z = 0, \quad (21)$$

$$\bar{n} \frac{\partial \bar{E}'}{\partial t} + \frac{\partial \Gamma'_{\bar{E}'}}{\partial p_\theta} + \Gamma'_{\bar{V}} \frac{\partial \bar{V}}{\partial p_\theta} + \Gamma_{\bar{n}} \frac{\partial \bar{E}'}{\partial p_\theta} + \bar{V} F_z = 0. \quad (22)$$

Here,  $\Gamma_{\bar{n}}$ ,  $\Gamma'_{\bar{V}}$ , and  $\Gamma'_{\bar{E}'}$  are the (scaled) fluxes of particles, axial momentum, and energy, respectively (the latter two being defined in a frame moving axially with mean fluid velocity  $\bar{V}$ ),

$$\Gamma_{\bar{n}}(p_\theta, t) = - \int d\theta dz dp_z f \frac{\partial \phi}{\partial \theta}, \quad (23)$$

$$\Gamma'_{\bar{V}}(p_\theta, t) = - \int d\theta dz dp_z p_z' f \frac{\partial \phi}{\partial \theta}, \quad (24)$$

$$\Gamma'_{\bar{E}'}(p_\theta, t) = - \int d\theta dz dp_z [H' - \bar{E}'] f \frac{\partial \phi}{\partial \theta}, \quad (25)$$

where  $p_z' = p_z - m\bar{V}$  and  $H' = p_z'^2/2m + \phi$  are the momentum and energy seen in the moving frame. Also,  $F_z$  is the axial force per unit volume (integrated over  $\theta$  and  $z$ ),

$$F_z(p_\theta, t) = - \int d\theta dz dp_z f \frac{\partial \phi}{\partial z}. \quad (26)$$

The scaled particle flux,  $\Gamma_{\bar{n}}$ , is related to the unscaled radial particle flux  $\Gamma_r$  via Eq. (9),

$$\Gamma_r = \left( \frac{c}{eBr} \right) \Gamma_{\bar{n}}. \quad (27)$$

This equation together with Eq. (20) implies that the density evolves according to the continuity equation

$$\frac{\partial \bar{n}}{\partial t} + \frac{1}{r} \frac{\partial}{\partial r} (r\Gamma_r) = 0. \quad (28)$$

Equations (21) and (22) have similar interpretations in terms of conservation of momentum and energy.

## B. Fluxes in the transport limit

The main object of this section is to derive expressions for the fluxes under various conditions. To obtain such expressions, we must solve the kinetic equation for the distribution function. The solution is found in the following “transport limit.” In this limit, the potential  $\phi$  is assumed to have the form,

$$\phi(\theta, p_\theta, z) = \phi_0(p_\theta, z) + \delta\phi(\theta, p_\theta, z), \quad (29)$$

where  $\phi_0$  is the azimuthally symmetric “equilibrium” potential energy, and  $\delta\phi$  is the field error, and it is assumed that

$$|\delta\phi| \ll \bar{T}. \quad (30)$$

Also, if  $\bar{V}$  is nonzero the transport limit also requires no  $z$ -dependence in  $\phi_0$ ,

$$\frac{\partial\phi_0}{\partial z} = 0 \quad \text{if } \bar{V} \neq 0. \quad (31)$$

These conditions allow a separation of time scales in the solution for  $f$ . On a relatively fast time scale of order  $\nu^{-1}$  (where  $\nu$  is the collision frequency),  $f$  approaches a quasi-equilibrium form that depends on time only parametrically through its dependence on  $\bar{n}$ ,  $\bar{V}$ , and  $\bar{E}$ . These three variables slowly evolve via the fluid equations (20)–(22), on a transport time scale that becomes arbitrarily long as  $|\delta\phi/\bar{T}| \rightarrow 0$ .

In the transport limit the distribution function is best represented as a product of two parts:

$$f = f_0(1 + g), \quad (32)$$

where  $g$  represents the nonadiabatic response to the field error, with  $g \ll 1$ , and

$$f_0 \equiv \frac{N(p_\theta, t) e^{-(H - \bar{V}p_z)/T_0}}{\sqrt{2\pi m T_0}} \quad (33)$$

is the adiabatic response, a Maxwellian with temperature  $T_0$  and arbitrary radial density profile. (Note that  $f_0$  depends on  $\delta\phi$  through  $H$  as  $e^{-\delta\phi/T_0}$ .)

Furthermore, we require that fluid quantities that are conserved in collisions are determined entirely by  $f_0$ ; that is,

$$\{\bar{n}, m\bar{V}, \bar{E}'\} = \int d\theta dz dp_z f_0 \{1, p_z, H'\}. \quad (34)$$

This requirement together with Eqs. (14)–(16) and (32) then implies that the perturbed distribution  $g$  is “orthogonal” to these conserved quantities,

$$\int d\theta dz dp_z f_0 g \{1, p_z, H'\} = \mathcal{O}. \quad (35)$$

The function  $N(p_\theta, t)$  appearing in  $f_0$  can be related to the  $\theta$ - and  $z$ -integrated density profile  $\bar{n}(p_\theta, t)$  by substituting Eq. (32) into Eq. (14) and applying Eq. (35),

$$\bar{n}(p_\theta, t) = N(p_\theta, t) e^{m\bar{V}^2/2T_0} \int d\theta dz e^{-\phi/T_0}. \quad (36)$$

Also, Eqs. (34) and (33) imply that  $T_0$  is related to  $\bar{E}'$  by

$$\bar{E}'(T_0, p_\theta) = \frac{T_0}{2} + \langle\phi\rangle(T_0, p_\theta), \quad (37)$$

where

$$\langle\phi\rangle(T_0, p_\theta) = \frac{\int d\theta dz e^{-\phi/T_0} \phi}{\int d\theta dz e^{-\phi/T_0}} \quad (38)$$

is the average of  $\phi$  over  $f_0$ . In other words,  $T_0$  is the temperature of an equilibrium system that has energy  $\bar{E}'$  per particle (as seen in the moving frame). This differs slightly from the temperature  $\bar{T}$  defined via the kinetic energy through Eq. (18). Comparing Eqs. (37) and (17) implies that

$$T_0 = \bar{T} + 2(\bar{\phi} - \langle\phi\rangle) = \bar{T} + \frac{2}{\bar{n}} \int d\theta dz dp_z f_0 g \phi. \quad (39)$$

Note that  $f_0$  does not itself drive fluxes, since  $f_0 \partial\phi/\partial\theta = -T_0^{-1} \partial f_0/\partial\theta$ , and  $f_0 \partial\phi/\partial z = -T_0^{-1} \partial f_0/\partial z$ . Thus, Eqs. (23)–(26) can be written as

$$\{\Gamma_{\bar{n}}, \Gamma'_{\bar{V}}, \Gamma'_{\bar{E}}\} = - \int d\theta dz dp_z f_0 g \frac{\partial\phi}{\partial\theta} \{1, p'_z, H' - \bar{E}'\} \quad (40)$$

and

$$F_z = - \int d\theta dz dp_z f_0 g \frac{\partial\phi}{\partial z}. \quad (41)$$

[In deriving the third component of Eq. (40) we have used the identity  $\int_0^{2\pi} d\theta \phi e^{-\phi/T_0} \partial\phi/\partial\theta = 0$ .]

An equation for  $g$  is obtained by substitution of Eq. (32) into Eq. (11), using  $\hat{C}f_0 = 0$ ,

$$\frac{\partial g f_0}{\partial t} + \frac{\partial f_0}{\partial t} + [g f_0, H] - \hat{C}_L(f_0, g) = -[f_0, H], \quad (42)$$

where  $\hat{C}_L$  is the collision operator found by linearizing  $\hat{C}f$  about  $f_0$ , assuming  $g \ll 1$ . In the transport limit, the first term on the left-hand side of Eq. (42) is negligible compared to the second term once  $g$  has rapidly evolved to its quasiequilibrium form with  $g \ll 1$ . We therefore neglect this term in what follows. The second term on the left-hand side can be evaluated directly using Eq. (33),

$$\frac{\partial f_0}{\partial t} = f_0 \left[ \frac{\dot{N}}{N} + \frac{p_z \dot{\bar{V}}}{T_0} + \left( \frac{H - p_z \bar{V}}{T_0} - \frac{1}{2} \right) \frac{\dot{T}_0}{T_0} \right]. \quad (43)$$

But Eq. (36) implies that

$$\frac{\dot{N}}{N} = \frac{\dot{\bar{n}}}{\bar{n}} - \frac{m\bar{V}\dot{\bar{V}}}{T_0} + \frac{\dot{T}_0}{T_0^2} \left( \frac{m\bar{V}^2}{2} - \langle\phi\rangle \right), \quad (44)$$

so that

$$\frac{\partial f_0}{\partial t} = f_0 \left[ \frac{\dot{\bar{n}}}{\bar{n}} + \frac{p'_z \dot{\bar{V}}}{T_0} + (H' - \bar{E}') \frac{\dot{T}_0}{T_0^2} \right]. \quad (45)$$

The time derivatives appearing in Eq. (45) can be evaluated using the fluid equations (20)–(22), along with Eq. (37). For example,  $\dot{\bar{n}} = -\partial\Gamma_{\bar{n}}/\partial p_\theta$ . If one then writes the fluxes in

terms of  $g$  using Eqs. (40) and (41), it is apparent that  $\partial f_0/\partial t$  can be written as a linear functional of  $g$ . In other words, Eq. (42) can be written as

$$\hat{L}g = s, \quad (46)$$

where the linear operator  $\hat{L}$  is defined as

$$\hat{L}g \equiv \frac{1}{f_0} \frac{\partial f_0}{\partial t} + [g, H] - gs - \hat{C}g, \quad (47)$$

$$\hat{C}g \equiv \frac{\hat{C}_L(f_0, g)}{f_0}, \quad (48)$$

and the source function  $s$  is

$$s \equiv -[f_0, H]/f_0. \quad (49)$$

This function is the source of the perturbed distribution  $g$  through Eq. (46), which in turn is the source of the transport fluxes through Eqs. (40) and (41).

The functional form of  $s$  follows by substitution of Eq. (33) into Eq. (49), using Eq. (36) to write  $N$  in terms of  $\bar{n}$ . The result is

$$s = \frac{\bar{V}}{T_0} \frac{\partial \phi}{\partial z} + \frac{1}{T_0} \frac{\partial \delta \phi}{\partial \theta} \left[ -\omega_r + p'_z \frac{\partial \bar{V}}{\partial p_\theta} + (H' - \bar{E}') \frac{1}{T_0} \frac{\partial T_0}{\partial p_\theta} \right], \quad (50)$$

where

$$\omega_r(p_\theta, t) = -\frac{\partial \langle \phi \rangle}{\partial p_\theta} - \frac{T_0}{\bar{n}} \frac{\partial \bar{n}}{\partial p_\theta} \quad (51)$$

is the mean fluid rotation frequency, consisting of a sum of  $\theta$  and  $z$ -averaged  $\mathbf{E} \times \mathbf{B}$  and diamagnetic drifts. In Eq. (50) we may replace  $\bar{V} \partial \phi / \partial z$  by  $\bar{V} \partial \delta \phi / \partial z$  since, by assumption,  $\bar{V} = 0$  if  $\partial \phi_0 / \partial z \neq 0$  [see Eq. (31)].

From Eq. (50), we see that nonzero  $s$ , and hence nonzero transport, is caused either by nonzero  $\omega_r$ ,  $\partial \bar{V} / \partial p_\theta$ , or  $\partial T_0 / \partial p_\theta$  in the presence of a field error  $\partial \delta \phi / \partial \theta$ ; or by nonzero  $\bar{V}$  in the presence of a  $z$ -electric field,  $-\partial \delta \phi / \partial z$ . In either case the transport limit, Eqs. (30) and (31) implies that  $s$  is of order  $\delta \phi / T_0 \ll 1$ , so that  $g \ll 1$ , consistent with our approximation of neglecting the first term on the left-hand side of Eq. (42).

### C. Formal solution for $g$

In order to solve Eq. (46) for  $g$ , we introduce the following inner product:

$$(g, h) \equiv \int d\theta dp_\theta dz dp_z f_0 g^* h, \quad (52)$$

and we define the adjoint operator  $\hat{L}^\dagger$  with respect to this inner product in the usual manner,<sup>27</sup>

$$(\hat{L}^\dagger f, g) \equiv (f, \hat{L}g). \quad (53)$$

The specific form for  $\hat{L}^\dagger$  is not needed here, but it can be found by applying an integration by parts to the right-hand side of Eq. (53). By assumption, boundary terms in the integration by parts are dropped since we restrict ourselves to

functions  $f$  and  $g$  with homogeneous boundary conditions.

Now consider eigenfunctions  $\psi_\alpha$  and  $\psi_\alpha^\dagger$  of  $\hat{L}$  and  $\hat{L}^\dagger$  that, respectively, satisfy

$$\hat{L}\psi_\alpha = \Lambda_\alpha \psi_\alpha \quad (54)$$

and

$$\hat{L}^\dagger \psi_\alpha^\dagger = \Lambda_\alpha^\dagger \psi_\alpha^\dagger, \quad (55)$$

subject to these same homogeneous boundary conditions, where  $\Lambda_\alpha$  and  $\Lambda_\alpha^\dagger$  are the corresponding eigenvalues. It is easily proven that for each eigenfunction  $\psi_\alpha$  there is a corresponding ‘‘left eigenfunction’’  $\psi_\alpha^\dagger$  such that

$$\Lambda_\alpha^\dagger = \Lambda_\alpha^*, \quad (56)$$

and furthermore, if  $\Lambda_\beta^\dagger \neq \Lambda_\alpha^*$  for some eigenfunctions  $\psi_\beta^\dagger$  and  $\psi_\alpha$ , then

$$(\psi_\beta^\dagger, \psi_\alpha) = 0. \quad (57)$$

Finally, we note that there is a set of left eigenfunctions  $\{\psi_{0\alpha}^\dagger\}$  for which  $\Lambda_\alpha^\dagger = 0$ . These eigenfunctions are

$$\{\psi_{0\alpha}^\dagger\} = [\delta(p_\theta - p_{\theta\alpha}), p'_z \delta(p_\theta - p_{\theta\alpha}), (H' - \bar{E}') \delta(p_\theta - p_{\theta\alpha})]. \quad (58)$$

This follows from taking  $f = \psi_{0\alpha}^\dagger$  and  $g$  any function in Eq. (53),

$$(\hat{L}^\dagger \psi_{0\alpha}^\dagger, g) = (\psi_{0\alpha}^\dagger, \hat{L}g). \quad (59)$$

However, this inner product is equivalent to taking fluid moments of  $\hat{L}g$ . Application of the fluid equations together with Eq. (45) shows that  $(\psi_{0\alpha}^\dagger, \hat{L}g) = 0$  for any function  $g$ , and therefore  $\hat{L}^\dagger \psi_{0\alpha}^\dagger = 0$ .

The corresponding eigenfunctions  $\{\psi_{0\alpha}\}$  have  $\Lambda_\alpha = 0$  according to Eqs. (55) and (56), and so are in the null space  $n$  of  $\hat{L}$ ; they constitute homogeneous solutions to Eq. (46) that also satisfy the aforementioned homogeneous boundary conditions. In what follows we assume that  $\{\psi_{0\alpha}\}$  spans the null space  $n$ .

Using Eqs. (54) and (57), the general solution to Eq. (46) may be written as a sum over the eigenfunctions,

$$g = \sum_\alpha' \frac{(\psi_\alpha^\dagger, s) \psi_\alpha}{\Lambda_\alpha (\psi_\alpha^\dagger, \psi_\alpha)} + \sum_{\alpha \in n} a_\alpha \psi_{0\alpha}, \quad (60)$$

where the  $a_\alpha$  are undetermined coefficients, and the prime on the first sum indicates that only eigenfunctions outside the null space are included (i.e.,  $\Lambda_\alpha \neq 0$ ). The coefficients  $a_\alpha$  are found by noting that, according to Eq. (35),

$$(\psi_{0\beta}^\dagger, g) = 0 \quad (61)$$

for every  $\beta \in n$ . Since by Eq. (57),  $(\psi_{0\beta}^\dagger, \psi_\alpha) = 0$  if  $\alpha \notin n$ , we obtain

$$\sum_{\alpha \in n} a_{\alpha}(\psi_{0\beta}^{\dagger}, \psi_{0\alpha}) = 0, \quad \forall \beta \in n, \quad (62)$$

and the only solution to this set of equations is  $a_{\alpha}=0$  (barring the possibility of degeneracies among the eigenfunctions). Therefore, the unique solution to Eq. (46) is

$$g = \sum_{\alpha} \frac{(\psi_{\alpha}^{\dagger}, s) \psi_{\alpha}}{\Lambda_{\alpha}(\psi_{\alpha}^{\dagger}, \psi_{\alpha})}. \quad (63)$$

Equation (63) is an elegant formal solution to Eq. (43), but can be difficult to implement in practice as it involves the determination of the set of left and right eigenfunctions for  $\hat{L}$ . Another approach that lends itself more easily to numerical solutions is to note that the  $f_0^{-1} \partial f_0 / \partial t$  term in  $\hat{L}$  can be written as

$$f_0^{-1} \partial f_0 / \partial t = \lambda_1(p_{\theta}, t) + p_z' \lambda_2(p_{\theta}, t) + H' \lambda_3(p_{\theta}, t), \quad (64)$$

where the coefficient functions  $\lambda_1$ ,  $\lambda_2$ , and  $\lambda_3$  are related to fluxes and forces via Eqs. (40), (41), (45), and (20)–(22). Let us call the rest of  $\hat{L}$  an operator  $\hat{L}_1$ ,

$$\hat{L}_1 g = \hat{L} g - f_0^{-1} \partial f_0 / \partial t = [g, H] - g s - \hat{C} g, \quad (65)$$

and write Eq. (46) as

$$\hat{L}_1 g = s - \lambda_1 - p_z' \lambda_2 - H' \lambda_3. \quad (66)$$

We can then solve for  $g$  as a sum of four terms,

$$g = \hat{L}_1^{-1} s - \hat{L}_1^{-1} \lambda_1 - \hat{L}_1^{-1} (p_z' \lambda_2) - \hat{L}_1^{-1} (H' \lambda_3). \quad (67)$$

Finally, the functions  $\lambda_1$ ,  $\lambda_2$ , and  $\lambda_3$  are determined by ensuring that  $g$  satisfy the three constraint equations (35).

The solution for  $g$  from either Eq. (63) or (67) can be used to determine transport fluxes using Eqs. (40) and (41). However, in order to relate these fluxes to transport coefficients, further approximations are necessary. These approximations are described in the following section.

#### D. The local approximation

In general, the transport fluxes, Eqs. (40) and (41), are not linearly proportional to the forcing functions  $\omega_r$ ,  $\bar{V}$ ,  $\partial T_0 / \partial p_{\theta}$ , and  $\partial \bar{V} / \partial p_{\theta}$  that appear in the source function  $s$  [see Eq. (50)]. Rather, the transport is a (generally nonlinear) functional of these four functions of  $p_{\theta}$ . This can be seen by cursory examination of Eq. (46); the forcing functions appear on both the left- and right-hand sides.

In order to simplify the solution for  $g$  and to extract transport coefficients, we make the following ‘‘local’’ approximation. When the Poisson bracket in Eq. (46) is expanded, the equation becomes

$$-\omega_E \frac{\partial g}{\partial \theta} - \frac{\partial \phi}{\partial \theta} \frac{\partial g}{\partial p_{\theta}} + v_z \frac{\partial g}{\partial z} - \frac{\partial \phi}{\partial z} \frac{\partial g}{\partial p_z} - g s - \hat{C} g + \frac{1}{f_0} \frac{\partial f_0}{\partial t} = s, \quad (68)$$

where  $\omega_E = -\partial \phi / \partial p_{\theta}$  is the  $\mathbf{E} \times \mathbf{B}$  rotation frequency. Noting that  $\delta \phi / T_b \ll 1$  in the transport limit, we drop the  $\partial \phi / \partial \theta \partial g / \partial p_{\theta}$  term from Eq. (68), and also replace  $\omega_E$  with the equilibrium rotation frequency  $\omega_0 = -\partial \phi_0 / \partial p_{\theta}$ . This ap-

proximation still allows particle trapping, although the orbit is modified in the  $(\theta, p_{\theta})$  plane.<sup>28</sup> The source function appearing on the left-hand side of Eq. (68) must also be modified so that the resulting operator has the symmetry properties necessary to satisfy Onsager relations. These modifications have only a small effect (of order  $\delta \phi / T$ ) on the solution for  $g$ . Equation (68) then becomes

$$\hat{L}_{\ell} g + \lambda_1 + \lambda_2 p_z' + \lambda_3 H' = s, \quad (69)$$

where we substituted Eq. (64) for  $\partial f_0 / \partial t$ , and where the local operator  $\hat{L}_{\ell}$  is defined as

$$\hat{L}_{\ell} = \hat{A} - \hat{C}, \quad (70)$$

and the operator  $\hat{A}$  is

$$\hat{A} = -\omega_0 \frac{\partial}{\partial \theta} + v_z \frac{\partial}{\partial z} - \frac{\partial \phi}{\partial z} \frac{\partial}{\partial p_z} + \frac{1}{2T_0} \left( \omega_0 \frac{\partial \phi}{\partial \theta} - \bar{V} \frac{\partial \phi}{\partial z} \right). \quad (71)$$

Equation (69) is linear in  $g$  and is local in  $p_{\theta}$ , which allows us to simplify the solution. We first note that  $s$  can be written as

$$s = s_i \mathcal{F}_i / T_0, \quad (72)$$

where the Einstein summation notation is used, the four source functions  $s_i$ ,  $i=0\dots 3$ , are defined as

$$\{s_0, s_1, s_2, s_3\} \equiv \left\{ \frac{\partial \phi}{\partial z}, \frac{\partial \phi}{\partial \theta}, p_z', \frac{\partial \phi}{\partial \theta} \frac{H' - \bar{E}'}{T_0} \frac{\partial \phi}{\partial \theta} \right\} \quad (73)$$

and the forcing functions  $\mathcal{F}_i$  are defined as

$$\{\mathcal{F}_0, \mathcal{F}_1, \mathcal{F}_2, \mathcal{F}_3\} \equiv \left\{ \bar{V}, -\omega_r, \frac{\partial \bar{V}}{\partial p_{\theta}}, \frac{\partial T_0}{\partial p_{\theta}} \right\}. \quad (74)$$

Since Eq. (69) is linear in  $g$  and since  $\mathcal{F}_i$  and  $\lambda_i$  are functions only of  $p_{\theta}$  and  $t$ , the solution to Eq. (69) can be written as

$$g = \frac{g_i \mathcal{F}_i}{T_0} - \lambda_i G_i, \quad (75)$$

where  $\mathbf{G} = \{G_1, G_2, G_3\}$  are solutions to

$$\hat{L}_{\ell} \mathbf{G} = \{1, p_z', H'\} \equiv \Phi, \quad (76)$$

and where  $\mathbf{g} = \{g_0, \dots, g_3\}$  are solutions to

$$\hat{L}_{\ell} \mathbf{g} = \mathbf{s}. \quad (77)$$

The constants  $\lambda_i$  are then determined by the constraint conditions (35). It is convenient to express these using an inner product,

$$(\Phi, \mathbf{g})_{p_{\theta}} = 0, \quad (78)$$

where this inner product is defined by its action on two functions  $g$  and  $h$ ,

$$(g, h)_{p_{\theta}} \equiv \int d\theta dz dp_z f_0 g^* h. \quad (79)$$

Substituting Eq. (75) into Eq. (78) and solving for  $\lambda_i$ , we may then write the solution for  $g$  as

$$g = \frac{1}{T_0}(g_j - G_k \alpha_{kj}) \mathcal{F}_j, \quad (80)$$

where the  $3 \times 4$  matrix  $\alpha_{kj}$  is defined by the solution to

$$(\Phi_i, G_k)_{p_\theta} \alpha_{kj} = (\Phi_i, g_j)_{p_\theta}, \quad i = 1, 2, 3. \quad (81)$$

Equation (80) shows that the perturbed distribution  $g$  is linearly proportional to the forcing functions in the local approximation, allowing us to define a  $4 \times 4$  matrix  $\boldsymbol{\mu}$  of transport coefficients. Substituting Eq. (80) into Eqs. (40) and (41) and noticing that the functions  $s_i$  also appear in the integral expressions for the fluxes, we find that the fluxes are given by

$$\{F_z, \Gamma_{\bar{n}}, \Gamma_{\bar{v}}, \Gamma_{\bar{E}}/T_0\} = -\boldsymbol{\mu} \cdot \mathcal{F}, \quad (82)$$

where the components of  $\mu_{ij}$  of the transport coefficient matrix  $\boldsymbol{\mu}$  are

$$\mu_{ij} = \frac{1}{T_0} [(s_i, g_j)_{p_\theta} - (s_i, G_k)_{p_\theta} \alpha_{kj}]. \quad (83)$$

Our convention will be that  $i$  and  $j$  run from 0 to 3, in keeping with the notation of Eqs. (73) and (74).

The coefficient  $\mu_{11}$  is of particular interest, as it is related to radial mobility and diffusive particle fluxes that will be measured in the simulations described in Sec. III. According to Eqs. (27) and (51), this transport coefficient is related to a  $z$  and  $\theta$ -averaged radial particle flux given by

$$\Gamma_r = \left( \frac{c}{eBr} \right) \mu_{11} \left( -\frac{\partial \langle \phi_0 \rangle}{\partial p_\theta} - \frac{T_0}{\bar{n}} \frac{\partial \bar{n}}{\partial p_\theta} \right). \quad (84)$$

Using Eq. (9) for  $p_\theta$  allows Eq. (84) to be written as a sum of a mobility and diffusive flux,

$$\Gamma_r = \mu_r \langle F_r \rangle - D_r \frac{\partial \bar{n}}{\partial r}, \quad (85)$$

where  $\langle F_r \rangle = -\partial \langle \phi_0 \rangle / \partial r$  is the mean equilibrium force in the radial direction,

$$D_r = \left( \frac{c}{eBr} \right)^2 \frac{T_0}{\bar{n}} \mu_{11} \quad (86)$$

is the radial diffusion coefficient and

$$\mu_r = \bar{n} D_r / T_0 \quad (87)$$

is the radial mobility coefficient.

However, this is not the whole story. Equation (82) implies that particle fluxes are also driven by gradients in the temperature and by  $\bar{V}$ . The full radial particle flux is

$$\Gamma_r = \mu_r \langle F_r \rangle - D_r \frac{\partial \bar{n}}{\partial r} - \left( \frac{c}{eBr} \right)^2 \left( \mu_{10} \bar{V} + \mu_{12} \frac{\partial \bar{V}}{\partial r} + \mu_{13} \frac{\partial T_0}{\partial r} \right). \quad (88)$$

In particular, temperature-gradient-driven radial particle flux is often neglected when interpreting experiments that study transport due to static field errors, since the mobility flux typically dominates over the particle flux driven by  $\partial T_0 / \partial r$ , unless  $\partial T_0 / \partial r$  is large. If one takes the rotation frequency to

be of order  $\omega_p^2 / 2\Omega_c$  (as in a non-neutral plasma), the ratio of the temperature-gradient-driven and mobility fluxes is  $(\mu_{13} / \mu_{11})(2\lambda_D^2 / r) \partial \ln T_0 / \partial r$ . On the other hand, for a plasma maintained in steady-state by a rotating-wall field error,<sup>33</sup> the mobility flux can be made arbitrarily small, in which case the temperature-gradient-driven particle flux cannot be neglected.

The coefficient  $\mu_{00}$  is also of interest, as it describes the drag force on a plasma moving at velocity  $\bar{V} \hat{z}$  with respect to a field error. This transport coefficient relates to Landau damping and current drive as seen in the wave frame. Here we see that the drag force is also affected by plasma rotation and by gradients:

$$F_z = - \left( \mu_{00} \bar{V} + \mu_{01} \omega_r + \mu_{02} \frac{\partial \bar{V}}{\partial p_\theta} + \mu_{03} \frac{\partial T_0}{\partial p_\theta} \right). \quad (89)$$

Note that plasma rotation can interact with a field error to generate a force in the axial direction through the transport coefficient  $\mu_{01}$ .

Radial energy and momentum transport is also driven by field errors, as described by the final two rows of the transport matrix. These energy and momentum fluxes are to be distinguished from those arising from collisions in the absence of field errors.

## E. Onsager relations

The transport coefficients  $\mu_{ij}$  are inter-related due to time-reversal symmetry of the dynamics underlying the local approximation.<sup>29</sup> To derive these relations, one defines the time reversed-distributions  $g_i^\dagger$  and  $G_i^\dagger$ , which satisfy equations obtained by reversing the sign of velocities and of the magnetic field,

$$\hat{L}_\ell^\dagger g_i^\dagger = s_i^\dagger, \quad (90)$$

$$\hat{L}_\ell^\dagger G_i^\dagger = \Phi_i^\dagger, \quad (91)$$

where

$$\hat{L}_\ell^\dagger = -\hat{A} - \hat{C}, \quad (92)$$

$$\mathbf{s}^\dagger = \left\{ \frac{\partial \phi}{\partial z}, \frac{\partial \phi}{\partial \theta}, -p'_z \frac{\partial \phi}{\partial \theta}, \frac{H' - \bar{E}'}{T_0} \frac{\partial \phi}{\partial \theta} \right\}, \quad (93)$$

and

$$\Phi^\dagger = \{1, -p'_z, H'\}. \quad (94)$$

Time-reversed transport coefficients  $\mu_{ij}^\dagger$  are obtained from the time-reversed version of Eq. (83),

$$\mu_{ij}^\dagger = \frac{1}{T_0} [(s_i^\dagger, g_j^\dagger)_{p_\theta} - (s_i^\dagger, G_k^\dagger)_{p_\theta} \alpha_{kj}^\dagger]. \quad (95)$$

Noting that  $s_i^\dagger = \pm s_i$ , with the lower sign only for  $i=2$ , and replacing  $s_i$  by  $\hat{L}_\ell g_i$  using Eq. (77), Eq. (95) becomes

$$\begin{aligned}\mu_{ij}^\dagger &= \pm \frac{1}{T_0} [(\hat{L}_\ell g_i, g_j^\dagger)_{p_\theta} - (\hat{L}_\ell g_i, G_k^\dagger)_{p_\theta} \alpha_{kj}^\dagger] \\ &= \pm \frac{1}{T_0} [(g_i, \hat{L}_\ell^\dagger g_j^\dagger)_{p_\theta} - (g_i, \hat{L}_\ell^\dagger G_k^\dagger)_{p_\theta} \alpha_{kj}^\dagger].\end{aligned}\quad (96)$$

In the second line we introduce the adjoint operator to  $\hat{L}_\ell$ , and note that by construction this adjoint operator is the time-reversal of  $\hat{L}_\ell$ , given by Eq. (92). Then Eqs. (90) and (91) imply

$$\mu_{ij}^\dagger = \pm \frac{1}{T_0} [(g_i, s_j^\dagger)_{p_\theta} - (g_i, \Phi_k^\dagger)_{p_\theta} \alpha_{kj}^\dagger].\quad (97)$$

Taking the case  $j \neq 2$  so that  $s_j^\dagger = s_j$ , and using Eq. (83) yields

$$\mu_{ij}^\dagger = \pm \mu_{ji} \pm \frac{1}{T_0} [(s_j^\dagger, G_k)_{p_\theta} \alpha_{ki} - (g_i, \Phi_k^\dagger)_{p_\theta} \alpha_{kj}^\dagger].\quad (98)$$

Substituting Eq. (90) for  $s_j^\dagger$  and applying the adjoint operation yields

$$\mu_{ij}^\dagger = \pm \mu_{ji} \pm \frac{1}{T_0} [(g_j^\dagger, \Phi_k)_{p_\theta} \alpha_{ki} - (g_i, \Phi_k^\dagger)_{p_\theta} \alpha_{kj}^\dagger], j \neq 2.\quad (99)$$

Substituting Eq. (81) for the two inner products, using  $\Phi_k^\dagger = \pm \Phi_k$ , yields

$$\mu_{ij}^\dagger = \pm \mu_{ji} \pm \frac{1}{T_0} [(\Phi_k, G_\ell^\dagger)_{p_\theta} \alpha_{\ell j}^\dagger \alpha_{ki} - (\Phi_k^\dagger, G_\ell)_{p_\theta} \alpha_{\ell i} \alpha_{kj}^\dagger].\quad (100)$$

However, Eqs. (76) and (91) imply that  $(\Phi_k, G_\ell^\dagger)_{p_\theta} = (\Phi_\ell^\dagger, G_k)_{p_\theta}$ . Since  $k$  and  $\ell$  are both dummy variables, there is a cancellation, leaving

$$\mu_{ij}^\dagger = \mu_{ji}\quad (101)$$

if both  $i$  and  $j$  are unequal to 2 and

$$\mu_{2j}^\dagger = -\mu_{j2}\quad (102)$$

if  $j \neq 2$ . By similar means, one finds for  $i=j=2$  that

$$\mu_{22}^\dagger = \mu_{22}.\quad (103)$$

Equations (101)–(103) are the Onsager relations for electrostatic field-error transport.

A separate reflection symmetry further simplifies the transport coefficient matrix in some cases. The operator  $\hat{L}_\ell$  has the property that  $\hat{L}_\ell^\dagger$  equals  $\hat{L}_\ell$  when viewed under reflected coordinates  $\theta \rightarrow \pi + \theta$ ,  $z \rightarrow -z$ , provided that the potential is symmetric under this reflection.

A similar reflection symmetry exists in the components  $s_i$  of the source function, which leads to the result that, for reflection-symmetric potentials,

$$\mu_{ij}^\dagger = \mu_{ij}\quad (104)$$

if both  $i$  and  $j$  are unequal to 2 or both  $i$  and  $j$  equal 2, and

$$\mu_{2j}^\dagger = -\mu_{2j},\quad (105)$$

$$\mu_{j2}^\dagger = -\mu_{j2}$$

for  $j$  unequal to 2.

When combined with the Onsager relations, this reflection symmetry leads to the simple result

$$\mu_{ij} = \mu_{ji}\quad (106)$$

for all  $i$  and  $j$ . Even if the potential does not have the required reflection symmetry, one can show that Eq. (106) is still satisfied in the linear response regime, where the kinetic equation for  $g$  can be linearized in  $\delta\phi$ .

## F. Entropy

The plasma entropy  $S$  also provides useful information concerning transport coefficients.<sup>1,24</sup> The entropy is defined as

$$S = - \int d\Gamma f \ln f,\quad (107)$$

where  $d\Gamma$  is the phase-space element  $dz dp_z d\theta dp_\theta$ . The rate of change of  $S$  is determined by the evolution of  $f$ ,

$$\begin{aligned}\dot{S} &= - \int d\Gamma \frac{\partial f}{\partial t} (\ln f + 1) \\ &= \int d\Gamma ([f \ln f, H] - (\ln f + 1) \hat{C}f) \\ &= - \int d\Gamma \ln f \hat{C}f.\end{aligned}\quad (108)$$

In the second line we used Eq. (11) for  $\partial f / \partial t$ , along with the identity

$$\int d\Gamma [f, g] = 0,$$

for any phase functions  $f$  and  $g$  that vanish at infinity; and in deriving the third line we used Eq. (13).

In the local approximation, Eq. (108) can be used to place bounds on the transport coefficients. Writing  $f = f_0(1 + g)$  and expanding Eq. (108) to second order in  $g$  yields the expression

$$\dot{S} = - \int d\Gamma f_0 g \hat{C}g + O(g^3).\quad (109)$$

In the local approximation it is useful to consider the rate of change of entropy density, defined as

$$\dot{S}(p_\theta, t) = - \int dz dp_z d\theta f_0 g \hat{C}g.\quad (110)$$

Substituting Eq. (69) and using and the constraint equation (78) yields

$$\dot{S} = - (g, \hat{A}g - s)_{p_\theta}.\quad (111)$$

However,  $(g, \hat{A}g)_{p_\theta} = 0$  because  $\hat{A}$  is an anti-Hermitian operator (one whose adjoint  $\hat{A}^\dagger$  equals  $-\hat{A}$ ). Therefore,

$$\dot{S} = (g, s)_{p_\theta}. \quad (112)$$

Substituting for  $g$  and  $s$  using Eqs. (72), (80), and (83) yields

$$\dot{S} = \frac{\mu_{ij} \mathcal{F}_i \mathcal{F}_j}{T_0}. \quad (113)$$

The second law then implies that

$$\mu_{ii} \geq 0 \quad \text{and} \quad (114a)$$

$$4\mu_{ii}\mu_{jj} \geq (\mu_{ij} + \mu_{ji})^2, \quad i \neq j. \quad (114b)$$

Also, note that when the Onsager relations, Eqs. (101)–(103), are applied, Eq. (113) implies that  $\dot{S}^\dagger = \dot{S}$ . As one might expect, time reversal has no effect on entropy production.

Finally, we note that it is possible to couch Eq. (69) as a variational principle involving the entropy production rate.<sup>1,24,30</sup> This can be useful in obtaining numerical solutions for the transport coefficients. However, here we solve Eq. (69) directly rather than employing a variational procedure. For completeness, the variational formulation is provided in Appendix A.

## G. Uniqueness

Implicit in the preceding derivation of the transport coefficients is that the solution for the perturbed distribution function is unique. We prove this here, by obtaining a logical contradiction under the hypothesis that the solution is not unique.

Let  $g_1$  and  $g_2$  be two different solutions to  $\hat{L}_\ell g = s$  for some source function  $s$ . Then the difference  $\Delta g = g_1 - g_2$  satisfies the homogeneous equation  $\hat{L}_\ell \Delta g = 0$ . We prove that there is no nontrivial solution to this equation by considering the inner product  $(\Delta g, \hat{L}_\ell \Delta g)_{p_\theta}$ . Using Eq. (70) for  $\hat{L}_\ell$ , this inner product can be written as

$$(\Delta g, \hat{L}_\ell \Delta g)_{p_\theta} = (\Delta g, \hat{A} \Delta g)_{p_\theta} - (\Delta g, \hat{C} \Delta g)_{p_\theta}. \quad (115)$$

However, the anti-Hermitian nature of  $\hat{A}$  implies that the first inner product on the right-hand side vanishes. The second inner product,  $-(\Delta g, \hat{C} \Delta g)_{p_\theta}$ , is non-negative by the second law of thermodynamics; see Eq. (110). Thus,

$$(\Delta g, \hat{L}_\ell \Delta g)_{p_\theta} = -(\Delta g, \hat{C} \Delta g)_{p_\theta} \geq 0, \quad (116)$$

with equality only for trivial distributions that do not affect the entropy, i.e.,  $\Delta g = 1$ ,  $p'_z$  or  $H'$ . These functions are not allowed by the constraint conditions, Eq. (35). Since  $(\Delta g, \hat{L}_\ell \Delta g)_{p_\theta}$  must be greater than zero for any nontrivial  $\Delta g$ , there are no such functions that satisfy  $\hat{L}_\ell \Delta g = 0$ . Therefore, the solution to  $\hat{L}_\ell \Delta g = 0$  has only the trivial solution  $\Delta g = 0$ , and this in turn implies that the solution for  $g$  is unique.

## H. Nonconservative collisions

The previous results can be modified to allow collision operators that do not conserve energy or momentum, but still conserve the particle number. An example of such an operator is the Fokker–Planck operator

$$\hat{C}f = D \frac{\partial}{\partial p_z} \left( \frac{\partial f}{\partial p_z} + \frac{p_z - mV_b}{mT_b} f \right), \quad (117)$$

where  $D$ ,  $T_b$ , and  $V_b$  are given functions of  $p_\theta$ . We will couch the following discussion in terms of this operator since it will be used in numerical simulations described in the next section. Physically, this operator describes collisions with a background species at fixed temperature  $T_b(p_\theta)$ , moving with axial velocity  $V_b(p_\theta)$ .

The theory of transport due to these nonconservative collisions follows the same approach as the previous analysis. Here, however, it now is best to define  $f_0$  in terms of  $V_b$  and  $T_b$  rather than  $\bar{V}$  and  $T_0$ , so that  $\hat{C}f_0 = 0$ ,

$$f_0 = \frac{N(p_\theta, t) e^{-(H - p_z V_b)/T_b}}{\sqrt{2\pi m T_b}}. \quad (118)$$

Since energy and momentum are not conserved, it is necessary only to ensure that  $\bar{n} = \int d\theta dz dp_z f_0$ . Thus, constraint equations (35) are replaced by the single condition

$$\int d\theta dz dp_z f_0 g = 0. \quad (119)$$

Also,  $\partial f_0 / \partial t = \dot{N} f_0 / N$  so  $\lambda_2$  and  $\lambda_3$  can be set to zero in Eq. (64). Dissipative momentum and energy fluxes are then defined in a frame moving with velocity  $V_b$  rather than  $\bar{V}$ , and are in terms of the temperature  $T_b$  rather than  $T_0$ ,

$$\{\Gamma''_{\bar{V}}, \Gamma''_{\bar{E}}\} \equiv \int d\theta dz dp_z f_0 g \frac{\partial \phi}{\partial z} \{p''_z, H'' - \bar{E}''\}, \quad (120)$$

where  $p''_z = p_z - mV_b$ ,  $H'' = p''_z{}^2 / 2m + \phi$ , and  $\bar{E}'' \equiv T_b / 2 + \langle \phi \rangle$ . Note that these fluxes differ from those appearing in the fluid equations,

$$\Gamma'_{\bar{V}} = \Gamma''_{\bar{V}} + m\Gamma_{\bar{n}}(V_b - \bar{V}), \quad (121)$$

$$\Gamma'_{\bar{E}} = \Gamma''_{\bar{E}} + \Gamma_{\bar{n}} \left[ \bar{E}'' - \bar{E}' + m \frac{(V_b - \bar{V})^2}{2} \right] + \Gamma''_{\bar{V}}(V_b - \bar{V}). \quad (122)$$

The definitions of particle flux  $\Gamma_{\bar{n}}$  and the force  $F_z$  remain unchanged.

The operator  $\hat{A}$ , the forcing functions  $\mathcal{F}_i$ , and the source functions  $s_i$  are also defined in terms of  $V_b$  and  $T_b$  rather than  $\bar{V}$  and  $T_0$ ,

$$\hat{A} = -\omega_0 \frac{\partial}{\partial \theta} + v_z \frac{\partial}{\partial z} - \frac{\partial \phi}{\partial z} \frac{\partial}{\partial p_z} + \frac{1}{2T_b} \left( \omega_0 \frac{\partial \phi}{\partial \theta} - V_b \frac{\partial \phi}{\partial z} \right), \quad (123)$$

$$\mathcal{F} = \left\{ V_b, -\omega_r, \frac{\partial V_b}{\partial p_\theta}, \frac{\partial T_b}{\partial p_\theta} \right\}, \quad (124)$$

and

$$\mathbf{s} = \left\{ \frac{\partial \phi}{\partial z}, \frac{\partial \phi}{\partial \theta}, p_z'', \frac{\partial \phi}{\partial \theta}, \frac{(H'' - \bar{E}'')}{T_b}, \frac{\partial \phi}{\partial \theta} \right\}. \quad (125)$$

With these definitions the solution of the transport equation for  $g$  is

$$g = g_i \mathcal{F}_i - \lambda_1 G_1, \quad (126)$$

where, as before,

$$\hat{L}_\ell g_i = s_i, \quad (127)$$

$$\hat{L}_\ell G_1 = 1, \quad (128)$$

and where  $\lambda_1$  is chosen to satisfy Eq. (119),

$$\lambda_1 = \frac{(1, g_i)_{p_\theta} \mathcal{F}_i}{(1, G_1)_{p_\theta}}. \quad (129)$$

Fluxes can then be related to forces via a new transport matrix,

$$\{F_z, \Gamma_{\bar{n}}, \Gamma_{\bar{v}}, \Gamma_{\bar{E}}''/T_b\} = -\boldsymbol{\mu} \cdot \mathcal{F}, \quad (130)$$

where

$$\mu_{ij} = \frac{1}{T_b} \left[ (s_i, g_j)_{p_\theta} - \frac{(1, g_j)_{p_\theta}}{(1, G_1)_{p_\theta}} (s_i, G_1)_{p_\theta} \right]. \quad (131)$$

It is not difficult to show that these transport coefficients also satisfy the Onsager relations, Eqs. (101)–(103), and inequalities (114) also hold.

### III. SIMULATIONS

We have performed computer simulations of field error transport in order to test the theory. In these simulations the Hamiltonian equations of motion given by Eq. (8) are numerically integrated forward in time, but the parallel force law is modified in order to include a nonconservative collisional drag term,

$$\frac{dp_z}{dt} = -\frac{\partial \phi}{\partial z} - m\nu(v_z - V_b), \quad (132)$$

where  $\nu$  is the collision frequency and  $V_b$  is a given background velocity. Both  $\nu$  and  $V_b$  are taken to be constant. The drift-kinetic equations of motion are integrated using a standard fourth-order Runge–Kutta algorithm with constant time step size  $\Delta t$ . To account for collisions, after each time step a random momentum  $\Delta p$ , uniformly distributed in the range  $-p_0 < \Delta p < p_0$ , is added to  $p_z$ . According to the theory of Langevin dynamics, this random momentum step combined with the drag force in Eq. (132) is equivalent to a Fokker–Planck collision operator acting on the particle distribution, given by Eq. (117). The temperature  $T_b$  is related to the simulation parameters via the Einstein relation

$$T_b = \frac{p_0^2}{6m\nu\Delta t}. \quad (133)$$

The collision operator does not conserve momentum or energy, but does of course conserve particle number.

The simulations follow  $N$  particles with random initial conditions. All particles are started at the same radius  $r_0$  but are distributed randomly in  $v_z$ ,  $z$ , and  $\theta$  according to the Boltzmann distribution  $\exp[-(H - p_z V_b)/T_b]$ .

To measure particle transport, the simulations follow two quantities: the mean change in radial position of the particles,

$$\langle \Delta r \rangle = N^{-1} \sum_{i=1}^N [r_i(t) - r_i(0)], \quad (134)$$

and the mean squared change in radial position,

$$\langle \Delta r^2 \rangle(t) = N^{-1} \sum_{i=1}^N [r_i(t) - r_i(0)]^2. \quad (135)$$

The mean position varies linearly with time over long times compared to the collision frequency but short compared to the time to change radial position by order  $r_0$ ; and its rate of change is related to the mobility coefficient  $\mu_r$  via

$$\bar{n} \frac{d}{dt} \langle \Delta r \rangle = \mu_r \langle F_r \rangle. \quad (136)$$

(This assumes that axial velocity and radial gradients in temperature can be neglected.) The mean square change in radial position is related to the radial diffusion coefficient,

$$\frac{d}{dt} [\langle \Delta r^2 \rangle - \langle \Delta r \rangle^2] = 2D_r. \quad (137)$$

Finally, both  $\mu_r$  and  $D_r$  are related to the transport coefficient  $\mu_{11}$  through Eqs. (86) and (87), so Eqs. (136) and (137) provide independent measurements of  $\mu_{11}$ . In simulations with  $N$  values of a few thousand,  $\langle \Delta r^2 \rangle$  is generally determined with less error than  $\langle \Delta r \rangle$ .

Other transport coefficients can also be measured in these simulations. In relation to current drive, the momentum fluid equation corresponding to the collision operator of Eq. (117) is

$$m\bar{n} \frac{\partial \bar{V}}{\partial t} + \frac{\partial \Gamma_{\bar{v}}'}{\partial p_\theta} + m\Gamma_{\bar{n}} \frac{\partial \bar{V}}{\partial p_\theta} - F_z = -m\bar{n}\nu(\bar{V} - V_b). \quad (138)$$

On the transport time scale,  $\bar{V}$  approaches an equilibrium with  $\partial \bar{V} / \partial t = 0$ . A measurement of  $\bar{V} - V_b$ , obtained by summing over all particles, then provides a measurement of  $F_z$ ,

$$F_z = N^{-1} \sum_{i=1}^N m\bar{n}\nu(v_i - V_b). \quad (139)$$

Comparison of the value of the right-hand side to Eq. (89) then yields information on various transport coefficients, such as  $\mu_{00}$  and  $\mu_{01}$ .

In principle, other transport coefficients driven by gradients in  $V_b$  and  $T_b$  can also be determined by simulations of the type described here. For example, the coefficient  $\mu_{13}$  can

be evaluated by measuring the radial drift velocity  $d\langle\Delta r\rangle/dt$  due to a temperature gradient. However, care must be taken to subtract out the mobility drift given by Eq. (136), and to account for other effects of the temperature gradient. In particular, the radial diffusion coefficient depends on temperature, and so a temperature gradient can create a radial drift due only to the diffusive term, since particles in a temperature gradient will diffuse at different rates depending on temperature, creating an overall radial drift. This can be seen by generalizing Eq. (136) to include temperature gradients, as found by integrating Eq. (88) over radius,

$$\frac{d}{dt}\langle\Delta r\rangle = \frac{\mu_r}{\bar{n}}\langle F_r\rangle + \left.\frac{\partial D_r}{\partial r}\right|_T + \left[\frac{\partial D_r}{\partial T} - \left(\frac{c}{eBr}\right)^2 \frac{\mu_{13}}{\bar{n}}\right] \frac{\partial T}{\partial r}. \quad (140)$$

#### IV. EXAMPLES

In this section we consider three examples of field error transport of increasing complexity: a plasma that is periodic in  $z$ ; a finite-length plasma; and a finite-length plasma to which an extra ‘‘squeeze’’ potential is added. In each case we calculate transport coefficients and then compare to simulations that measure some of these coefficients. In all three examples we use the nonconservative collision operator, Eq. (117).

##### A. Example 1: Periodic boundaries in $z$

In the first, simplest example, we assume periodic boundary conditions in  $z$  and a sinusoidal field error of amplitude  $\varepsilon(p_\theta)$  with axial wavenumber  $k$  and  $\theta$  wavenumber  $\ell$ . The Hamiltonian for the motion is

$$H = \frac{p_z^2}{2m} + \phi_0(p_\theta) + \varepsilon(p_\theta)\cos(\ell\theta + kz), \quad (141)$$

where  $\varepsilon/\bar{T} \ll 1$  is assumed. For this Hamiltonian, the motion is integrable due to the existence of a constant of the motion  $P$ , where

$$P = p_\theta - \ell p_z/k. \quad (142)$$

Consequently, a confined thermal equilibrium exists with a Boltzmann distribution given by

$$f_{\text{eq}} = \frac{n_0}{\sqrt{2\pi m T_b}} \exp[-(H + \omega_r P)/T_b], \quad (143)$$

where  $n_0$  is a uniform density,  $\omega_r$  is the (uniform) fluid rotation frequency, and  $T_b$  is the (uniform) temperature. This distribution is a shifted Maxwellian moving with axial velocity  $V_{\text{eq}}$ , where

$$V_{\text{eq}} = \ell\omega_r/k. \quad (144)$$

If  $V_b = V_{\text{eq}}$  and  $f = f_{\text{eq}}$ , Eq. (11) implies that  $\partial f/\partial t = 0$  since  $[f_{\text{eq}}, H] = 0$  and  $\hat{C}f_{\text{eq}} = 0$ . One can also see that transport vanishes in thermal equilibrium from the form of the source function  $s$  for field errors with combined  $\theta$  and  $z$  dependence  $\ell\theta + kz$ ,

$$s = -\frac{1}{T} \frac{\partial \phi}{\partial \theta} \left( \omega_r - \frac{kV_b}{\ell} - p_z'' \frac{\partial V_b}{\partial p_\theta} - \frac{H'' - \bar{E}''}{T_b} \frac{\partial T_b}{\partial p_\theta} \right). \quad (145)$$

The source clearly vanishes when  $V_b = V_{\text{eq}}$  and  $T_b$  is uniform, the conditions for thermal equilibrium.

Note that  $\omega_r$  and  $V_b$  appear in  $s$  in the combination

$$\omega_r'' = \omega_r - kV_b/\ell, \quad (146)$$

the Doppler-shifted fluid rotation frequency. Since  $\partial/\partial z$  can be replaced by  $(k/\ell)\partial/\partial\theta$ , the flux equation (130) can be simplified to a  $3 \times 3$  form,

$$\{\Gamma_{\bar{n}}, \Gamma_{\bar{v}}, \Gamma_{\bar{E}}''/T_b\} = \hat{\boldsymbol{\mu}} \cdot \left\{ \omega_r'', \frac{\partial V_b}{\partial p_\theta}, \frac{\partial T_b}{\partial p_\theta} \right\}, \quad (147)$$

where  $\hat{\boldsymbol{\mu}}$  is a  $3 \times 3$  transport matrix obtained by dropping the leftmost column and topmost row of  $\boldsymbol{\mu}$ . In other words  $\hat{\mu}_{ij} = \mu_{ij}$  with  $i$  and  $j$  in the range 1–3. Also, the force  $F_z$  is related to  $\Gamma_{\bar{n}}$  via

$$F_z = \frac{k}{\ell} \Gamma_{\bar{n}}. \quad (148)$$

##### 1. Linear solution

If we linearize Eq. (127) in  $\delta\phi$ , using Eq. (141) and assuming that  $g$  is of order  $\delta\phi$ , the equation becomes

$$\left( -\omega_0 + \frac{kv_z}{\ell} \right) \frac{\partial \mathbf{g}}{\partial \theta} - \hat{C} \mathbf{g} = \mathbf{s}, \quad (149)$$

where

$$\mathbf{s} = \frac{\partial \phi}{\partial \theta} \{1, p_z'', p_z''^2/2mT_b - 1/2\}. \quad (150)$$

This equation can be solved by Fourier analysis in  $z$  and  $\theta$ , and expansion in momentum basis functions. Since Eqs. (117) and (48) imply that the operator  $\hat{C}$  is the Hermite operator,

$$\hat{C} \mathbf{g} = D \left( \frac{\partial^2 \mathbf{g}}{\partial p_z^2} - \frac{p_z''}{mT_b} \frac{\partial \mathbf{g}}{\partial p_z} \right), \quad (151)$$

we choose the momentum basis functions to be this operator's eigenfunctions, the Hermite polynomials  $H_{\bar{n}}(p_z''/\sqrt{2mT_b})$ ,

$$\mathbf{g} = \sum_{\bar{n}=0}^{\infty} \tilde{\mathbf{g}}_{\bar{n}} H_{\bar{n}} \left( \frac{p_z''}{\sqrt{2mT_b}} \right) e^{i(\ell\theta + kz)} + \text{c.c.} \quad (152)$$

Substituting this expansion into Eq. (149), multiplying by another Hermite polynomial  $H_{\bar{n}}(p_z''/\sqrt{2mT_b})$ , and integrating over  $p_z$  yields a matrix equation for the Fourier coefficients  $\tilde{\mathbf{g}}_{\bar{n}}$ ,

$$\sum_{\bar{n}=0}^{\infty} L_{\bar{n}\bar{m}} \tilde{\mathbf{g}}_{\bar{n}} = \tilde{\mathbf{s}}_{\bar{m}}, \quad (153)$$

where

$$\tilde{s}_n = \frac{\ell \varepsilon}{2} \{ \delta_{n0}, m\bar{v}/\sqrt{2}\delta_{n1}, \delta_{n2}/4 \}, \quad (154)$$

$$L_{n\bar{n}} = (-i\nu n - \ell \omega_0'') \delta_{n\bar{n}} + \frac{k\bar{v}}{\sqrt{2}} (\delta_{\bar{n},n-1} + 2\bar{n}\delta_{\bar{n},n+1}), \quad (155)$$

$\bar{v} = \sqrt{T_b/m}$  is the thermal speed,  $\omega_0'' = \omega_0 - kV_b/\ell$  is the Doppler-shifted  $\mathbf{E} \times \mathbf{B}$  rotation frequency, and  $\nu = D/mT_b$  is the collision frequency. A solution to Eq. (153) can be obtained numerically by matrix inversion. Since  $\ell$  and  $k$  are unequal to zero by assumption,  $\mathbf{g}$  automatically satisfies the constraint condition (119) so the linearized transport coefficients are

$$\mu_{ij} = \frac{1}{T_b} \int d\theta dz dp_z f_{00} s_i g_j, \quad (156)$$

where  $f_{00}$  is the linearized version of  $f_0$ ,

$$f_{00} = \frac{N}{\sqrt{2\pi m T_b}} e^{-(H_0 - V_b p_z)/T_b}, \quad (157)$$

and

$$H_0 = p_z^2/2m + \phi_0. \quad (158)$$

Using orthogonality of the Hermite polynomials and Fourier modes, Eq. (156) can be written as

$$\mu_{ij} = \frac{2}{T_b} \bar{n} \sum_{n=0}^{\infty} 2^n n! \text{Im}(\tilde{s}_{ni} \tilde{g}_{nj}). \quad (159)$$

Here  $i$  and  $j$  run from 1 to 3 and pick out one of the three components of the vectors  $\tilde{s}_n$  and  $\tilde{g}_n$  appearing in Eqs. (152) and (154). According to Eq. (154), in Eq. (159) only the  $n = i - 1$  term survives in the sum. Thus,

$$\mu_{ij} = 2\bar{n}/T_b 2^{i-1} (i-1)! \text{Im}(\tilde{s}_{i-1,i} \tilde{g}_{i-1,j}). \quad (160)$$

Also, for this example, several of the coefficients are related to one another. These relations are summarized by the matrix expression

$$\hat{\boldsymbol{\mu}} = \begin{pmatrix} \mu_{11} & \frac{m\ell\omega_0''}{k} \mu_{11} & \mu_{13} \\ \frac{m\ell\omega_0''}{k} \mu_{11} & \left(\frac{m\ell\omega_0''}{k}\right)^2 \mu_{11} & \frac{m\ell\omega_0''}{k} \mu_{13} \\ \mu_{13} & \frac{m\ell\omega_0''}{k} \mu_{13} & \mu_{33} \end{pmatrix}. \quad (161)$$

Thus, we only need calculate  $\mu_{11}$ ,  $\mu_{13}$ , and  $\mu_{33}$ . Furthermore, these coefficients, when suitably scaled, can be written as functions of only two dimensionless arguments,  $\ell\omega_0''/k\bar{v}$ , and  $\nu/k\bar{v}$ ,

$$\{\mu_{11}, \mu_{13}, \mu_{33}\} = \frac{\bar{n}}{T_b} \frac{\varepsilon^2 \ell^2}{k\bar{v}} \{ \bar{\mu}_{11}, \bar{\mu}_{13}, \bar{\mu}_{33} \}, \quad (162)$$

where  $\bar{\mu}_{11}$ ,  $\bar{\mu}_{13}$ , and  $\bar{\mu}_{33}$  are dimensionless functions of the two arguments. These three dimensionless functions are plotted in Figs. 1 and 2 versus  $\nu/k\bar{v}$  and  $\ell\omega_0''/k\bar{v}$ .

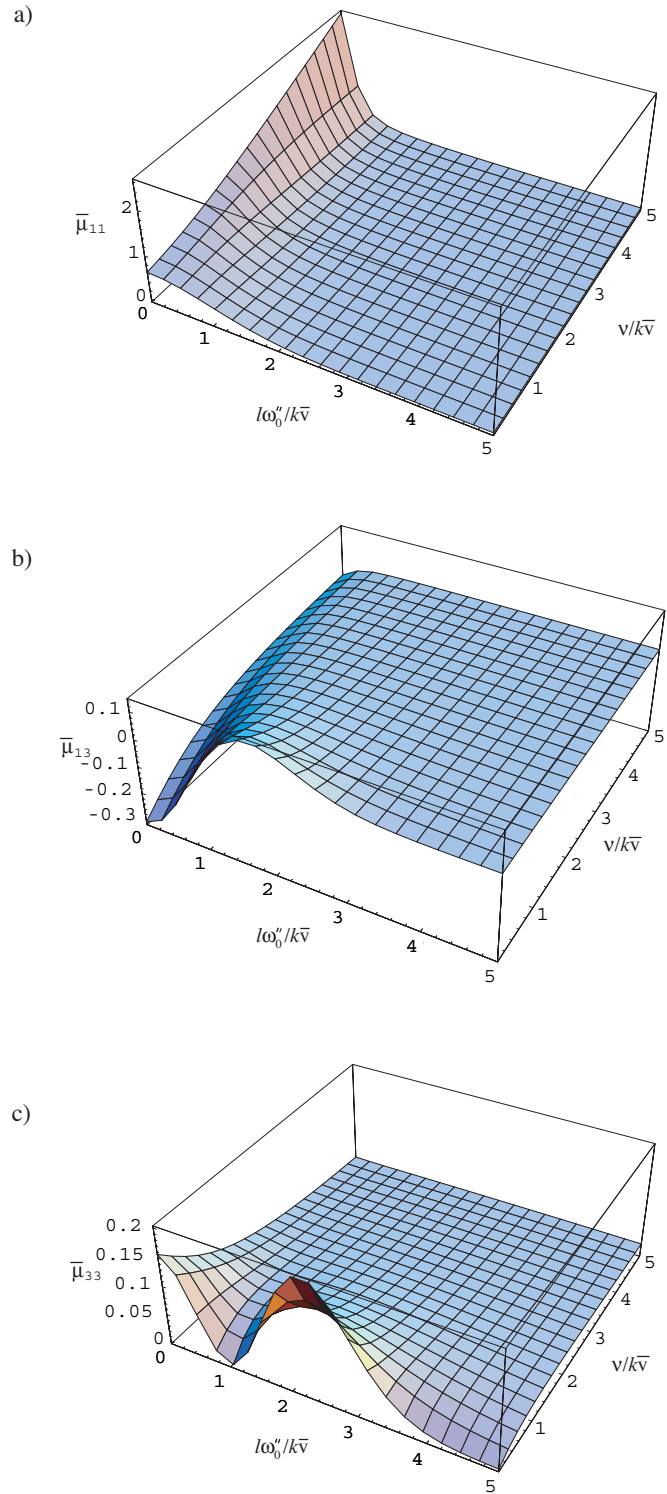


FIG. 1. (Color online) Surface plots of the three scaled transport coefficients  $\bar{\mu}_{11}$ ,  $\bar{\mu}_{13}$ , and  $\bar{\mu}_{33}$  as functions of collision frequency  $\nu$  and Doppler-shifted  $\mathbf{E} \times \mathbf{B}$  rotation frequency  $\omega_0''$  for the infinite-length plasma of example 1, using linearized theory.

In Fig. 1, taking the limit  $\nu/k\bar{v} \rightarrow 0$  yields the plateau-regime values of the scaled transport coefficients. The dependence of the coefficients on  $\ell\omega_0''/k\bar{v}$  will be derived in Sec. IV A 2. Note that while  $\mu_{11}$  and  $\mu_{33}$  are both non-negative, as required by Eq. (114a),  $\mu_{13} < 0$  for  $\ell\omega_0''/k\bar{v} < 1$ . For large  $\nu/k\bar{v}$  (i.e., the fluid regime), one can see from Fig. 1 that the

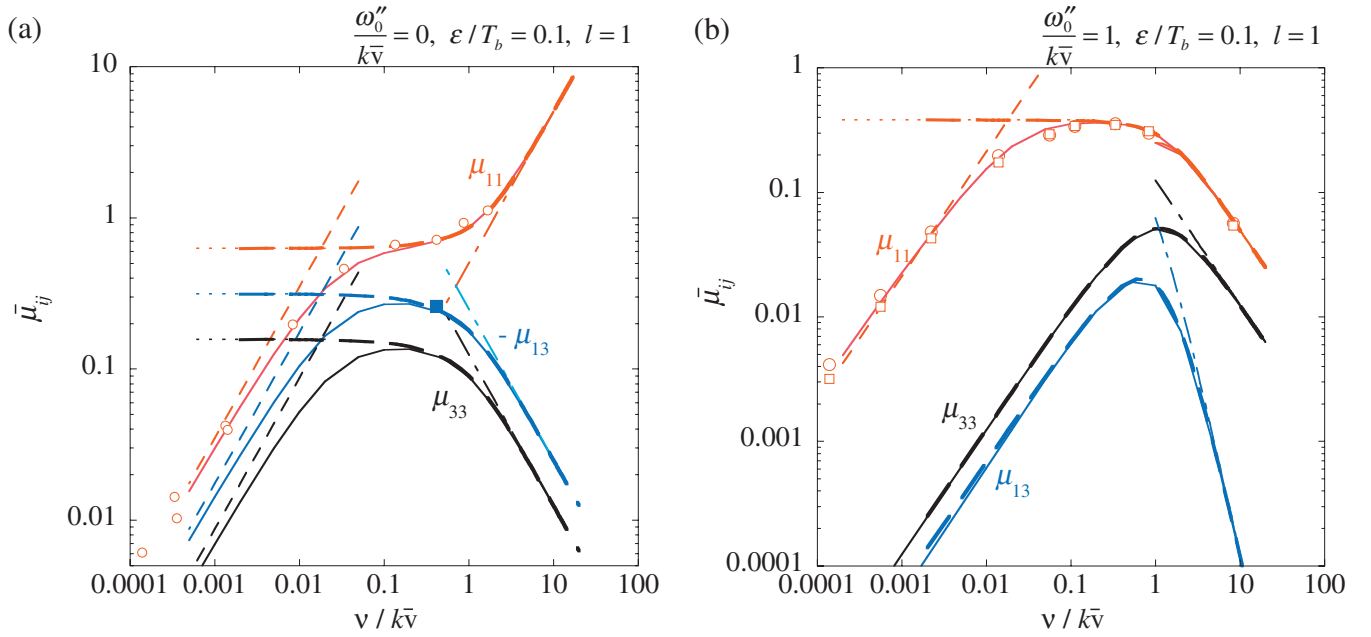


FIG. 2. (Color) The transport coefficients  $\mu_{11}$  (red),  $\mu_{13}$  (blue), and  $\mu_{33}$  (black) vs collision frequency  $\nu$ , scaled according to Eq. (162), for the infinite length plasma of example 1, with an  $\ell=1$  asymmetry with amplitude  $\varepsilon=0.1T_b$ , and for two different Doppler-shifted  $\mathbf{E} \times \mathbf{B}$  rotation frequencies. (a)  $\omega_0''/k\bar{v}=0$ ; (b)  $\omega_0''/k\bar{v}=1$ . Thick dashed lines display the linearized theory as in Fig. 1. Solid lines display the full nonlinear theory. Dotted lines are the plateau limit, dotted-dashed lines are the fluid limit, and the thin dashed lines are the banana limit. Open squares and circles are simulation results for  $\mu_{11}$  based on Eqs. (136) and (137), respectively. The single solid square in (a) is a simulation result for  $\mu_{13}$  using Eq. (140).

coefficients have no simple dependence on  $\nu/k\bar{v}$ . For example, for  $\omega_0''=0$ ,  $\mu_{11} \propto \nu$  for large  $\nu/k\bar{v}$  but for  $\omega_0'' \neq 0$ ,  $\mu_{11} \propto 1/\nu$ . The functional form of the coefficients in the fluid regime is derived in Sec. IV A 3.

In Fig. 2, the coefficients are plotted on a logarithmic scale for two values of  $\ell\omega_0''/k\bar{v}$  and for  $\varepsilon/T_b=0.1$  and compared to the results of simulations that measure  $\mu_{11}$  and (in one case)  $\mu_{13}$  as described in Sec. III. The linear theory described above is plotted as thick dashed lines, and agrees with the simulation results except when  $\nu/k\bar{v}$  is small. The discrepancy at small  $\nu/k\bar{v}$  occurs because the linear theory does not include trapping in banana orbits, which becomes important when Eq. (4) is satisfied. For  $\varepsilon/T_b=0.1$  this banana regime corresponds to  $\nu/k\bar{v} \leq 0.03$ , which is roughly where one observes a divergence between the linear theory and the simulations. A fully nonlinear numerical evaluation of the theory (given by the solid lines) and an asymptotic analytical theory (given by the thin dashed lines), both do a good job of matching the simulation results in the banana regime. These theory results are described in Sec. IV A 4.

## 2. Plateau regime

In the regime  $\nu \ll k\bar{v}$ , the linear theory results become independent of  $\nu$ . In this “plateau” regime the form of the collision operator is unimportant, so we replace  $\hat{C}g$  by  $-\nu g$  in Eq. (149) which allows the analytic solution,

$$\mathbf{g} = \frac{\ell\varepsilon}{2} \frac{e^{i(\ell\theta+kz)}}{k\nu_z - \ell\omega_0 - i\nu} \left\{ 1, p_z'', \frac{p_z''^2}{2mT_b} - \frac{1}{2} \right\} + \text{c.c.} \quad (163)$$

Substituting into Eq. (156) and applying the Plemelj formula to evaluate the  $p_z$  integral yields

$$\begin{aligned} (\bar{\mu}_{11}, \bar{\mu}_{13}, \bar{\mu}_{33}) &= \sqrt{\frac{\pi}{2}} \exp(-\ell^2 \omega_0''^2 / 2k^2 \bar{v}^2) \\ &\times \left\{ \frac{1}{2}, \frac{1}{4} \left[ \left( \frac{\ell\omega_0''}{k\bar{v}} \right)^2 - 1 \right], \frac{1}{8} \left[ \left( \frac{\ell\omega_0''}{k\bar{v}} \right)^2 - 1 \right]^2 \right\}. \end{aligned} \quad (164)$$

These limiting forms are plotted in Fig. 2. Their scaling agrees with Eq. (7). Note that if  $\ell\omega_0''/k\bar{v}=1$  [the case shown in Fig. 2(b)] the coefficients  $\mu_{13}$  and  $\mu_{33}$  vanish in the plateau regime.

## 3. Fluid regime

When  $\nu \gg k\bar{v}$ , the solution to Eq. (153) can be obtained as an expansion in  $1/\nu$ . The first three equations taken from Eq. (153) are

$$\sqrt{2}k\bar{v}\tilde{\mathbf{g}}_1 - \ell\omega_0''\tilde{\mathbf{g}}_0 = \frac{\ell\varepsilon}{2} \{1, 0, 0\}, \quad (165)$$

$$2\sqrt{2}k\bar{v}\tilde{\mathbf{g}}_2 - (\ell\omega_0'' + i\nu)\tilde{\mathbf{g}}_1 + \frac{k\bar{v}}{\sqrt{2}}\tilde{\mathbf{g}}_0 = \frac{\ell\varepsilon}{2} \left\{ 0, \frac{m\bar{v}}{\sqrt{2}}, 0 \right\}, \quad (166)$$

$$3\sqrt{2}k\bar{v}\tilde{\mathbf{g}}_3 - (\ell\omega_0'' + 2i\nu)\tilde{\mathbf{g}}_2 + \frac{k\bar{v}}{\sqrt{2}}\tilde{\mathbf{g}}_1 = \frac{\ell\varepsilon}{2} \{0, 0, 1/4\}. \quad (167)$$

These equations can be thought of as equations for the nonadiabatic response to the field error of the density, fluid velocity, and temperature, respectively. The form of these equations implies that  $\tilde{g}_n = O(1/\nu) \times \tilde{g}_{n-1}$ , and so for large  $\nu$  it is acceptable to drop higher  $n$  terms. For  $\mu_{11}$ , we need keep

only  $\tilde{\mathbf{g}}_0$  and  $\tilde{\mathbf{g}}_1$ , setting  $\tilde{\mathbf{g}}_n$  zero for  $n \geq 2$ . The solution of Eqs. (165) and (166) is then

$$\tilde{\mathbf{g}}_0 = \frac{\ell \varepsilon}{2} \frac{\{\ell \omega_0'' + i\nu, k\bar{\nu}, 0\}}{k^2 \bar{\nu}^2 - \ell \omega_0''(\ell \omega_0'' + i\nu)}, \quad (168)$$

$$\tilde{\mathbf{g}}_1 = \frac{\ell \varepsilon}{2\sqrt{2}} \frac{\{k\bar{\nu}, -\ell \omega_0'', 0\}}{k^2 \bar{\nu}^2 - \ell \omega_0''(\ell \omega_0'' + i\nu)}. \quad (169)$$

When applied to Eq. (159) we obtain, after simplification by dropping terms of higher order in  $1/\nu$ ,

$$\mu_{11} = \frac{\bar{n}}{2T_b} \ell^2 \varepsilon^2 \frac{k^2 \bar{\nu}^2 \nu}{\ell^2 \omega_0''^2 \nu^2 + k^4 \bar{\nu}^4}. \quad (170)$$

For  $\mu_{13}$  and  $\mu_{33}$ , we must also keep  $\tilde{\mathbf{g}}_2$ , but may set  $\tilde{\mathbf{g}}_3=0$  in Eq. (167). The solution yields, to lowest order in  $1/\nu$ ,

$$\mu_{13} = -\frac{\bar{n}}{8T_b} \ell^2 \varepsilon^2 \frac{k^2 \bar{\nu}^2}{\nu} \frac{2k^2 \bar{\nu}^2 - 3\ell^2 \omega_0''^2}{\ell^2 \omega_0''^2 \nu^2 + k^4 \bar{\nu}^4}, \quad (171)$$

and

$$\mu_{33} = \frac{\bar{n}}{8T_b} \frac{\ell^2 \varepsilon^2}{\nu}. \quad (172)$$

These functions are plotted in Fig. 2, and agree with the general linear theory when  $\nu/k\bar{\nu} \gg 1$ . It should be noted however that the functional form of these coefficients depends on the detailed form of the collision operator. Here we employed a Fokker–Planck operator that does not conserve momentum or energy. An energy conserving operator would give different results in the fluid regime. An example is worked out in Appendix B for the case of the Dougherty collision operator.<sup>31</sup>

#### 4. Banana regime

When the collision frequency is sufficiently small, such that Eq. (4) is satisfied, the previous linear analysis of the transport coefficients is no longer valid. As we discussed in the Introduction, the effect of particles trapped, or nearly trapped, in the potential wells of the field error then dominates the transport.

Here we present an asymptotic analysis of the transport in this regime, valid for  $\nu/k\bar{\nu} \rightarrow 0$ . The approach we use is similar to that taken by many previous authors; for example, for the case of a collisionally damped BGK wave,<sup>13</sup> and for the case of tokamak or stellarator transport.<sup>2,24</sup> The perturbed distribution functions  $g_i$ ,  $i=1,2,3$  satisfy  $\hat{L}_\ell g_i = s_i$ , which when written out in full becomes

$$\begin{aligned} & \left( \frac{kp_z''}{m\ell} - \omega_0'' \right) \frac{\partial \mathbf{g}}{\partial \theta} - \frac{k}{\ell} \frac{\partial \phi}{\partial \theta} \frac{\partial \mathbf{g}}{\partial p_z''} + \frac{\alpha}{T_b} \frac{\partial \phi}{\partial \theta} \mathbf{g} \\ & - D \left( \frac{\partial^2 \mathbf{g}}{\partial p_z''^2} - \frac{p_z''}{mT_b} \frac{\partial \mathbf{g}}{\partial p_z''} \right) = \frac{\partial \phi}{\partial \theta} \left\{ 1, p_z'', \frac{H'' - \bar{E}''}{T_b} \right\}. \end{aligned} \quad (173)$$

Here we have chosen Eq. (151) as a specific form for the collision operator. We have also introduced the parameter  $\alpha = \omega_0''/2$ . Recall that in Sec. II D the value of this parameter

was chosen so that  $\hat{L}_\ell$  satisfied Onsager symmetries, using the argument that changes in its value have a negligible effect on transport. We will prove this to be the case by allowing  $\alpha$  to be a free parameter in the equations, and showing that the results are independent of  $\alpha$  to lowest order in  $\varepsilon$ .

The source functions on the right-hand side of Eq. (173) can be eliminated or reduced in magnitude by means of the following substitution:

$$\mathbf{g} = \left[ \frac{T_b}{\alpha}, \frac{T_b}{\alpha} \left( p_z'' + \frac{kT_b}{\ell \alpha} \right), \frac{1}{\alpha} (H'' - \bar{E}'') + \frac{T_b \omega_0}{\alpha^2} \right] + \Delta \mathbf{g}, \quad (174)$$

implying that  $\Delta \mathbf{g}$  satisfies

$$\begin{aligned} & \left( \frac{kp_z''}{\ell m} - \omega_0'' \right) \frac{\partial \Delta \mathbf{g}}{\partial \theta} - \frac{k}{\ell} \frac{\partial \phi}{\partial \theta} \frac{\partial \Delta \mathbf{g}}{\partial p_z''} + \frac{\alpha}{T_b} \frac{\partial \phi}{\partial \theta} \Delta \mathbf{g} \\ & - D \left( \frac{\partial^2 \Delta \mathbf{g}}{\partial p_z''^2} - \frac{p_z''}{mT_b} \frac{\partial \Delta \mathbf{g}}{\partial p_z''} \right) \\ & = \left\{ 0, -\frac{Dp_z''}{m\alpha}, -\frac{D}{m\alpha} \left( \frac{p_z''^2}{mT_b} - 1 \right) \right\}. \end{aligned} \quad (175)$$

Before proceeding further, we introduce scaled variables  $\hat{\omega} = \ell \omega_0''/k\bar{\nu}$ ,  $\hat{\alpha} = \ell \alpha/k\bar{\nu}$ ,  $\hat{\nu} = \ell D/mT_b k\bar{\nu}$ ,  $\hat{\phi} = \phi/T_b$ ,  $\hat{\varepsilon} = \varepsilon/T_b$ , and  $\hat{p} = p_z''/m\bar{\nu} - \hat{\omega}$ , where  $\bar{\nu} = \sqrt{T_b/m}$  is the thermal speed. We also introduce a transformation of  $\Delta \mathbf{g}$  via

$$\Delta \mathbf{g} = \frac{\ell m \bar{\nu}}{k} e^{\hat{\alpha} \hat{p}} \mathbf{h}(\theta, \hat{p}). \quad (176)$$

The equation for  $\mathbf{h}$  is

$$\begin{aligned} & \hat{p} \frac{\partial \mathbf{h}}{\partial \theta} - \frac{\partial \hat{\phi}}{\partial \theta} \frac{\partial \mathbf{h}}{\partial \hat{p}} - \hat{\nu} \left[ \frac{\partial^2 \mathbf{h}}{\partial \hat{p}^2} + (2\hat{\alpha} - \hat{\omega} - \hat{p}) \frac{\partial \mathbf{h}}{\partial \hat{p}} \right. \\ & \left. + \hat{\alpha}(\hat{\alpha} - \hat{\omega} - \hat{p}) \mathbf{h} \right] = -\frac{\hat{\nu}}{\hat{\alpha}} e^{-\hat{\alpha} \hat{p}} \{0, m\bar{\nu}(\hat{p} + \hat{\omega}), (\hat{p} + \hat{\omega})^2 - 1\}. \end{aligned} \quad (177)$$

Introducing the scaled energy  $E$ , where

$$E = \frac{\hat{p}^2}{2} + \hat{\phi}(\theta), \quad (178)$$

we change variables from  $\hat{p}$  to  $E$  in Eq. (177), yielding

$$\begin{aligned} & \hat{p} \frac{\partial \mathbf{h}}{\partial \theta} \Big|_E - \hat{\nu} \hat{p} \left[ \frac{\partial}{\partial E} \hat{p} \frac{\partial \mathbf{h}}{\partial E} + (2\hat{\alpha} - \hat{\omega} - \hat{p}) \frac{\partial \mathbf{h}}{\partial E} \right. \\ & \left. + \hat{\alpha}(\hat{\alpha} - \hat{\omega} - \hat{p}) \mathbf{h} \right] \\ & = -\frac{\hat{\nu}}{\hat{\alpha}} e^{-\hat{\alpha} \hat{p}} \{0, (\hat{p} + \hat{\omega}), (\hat{p} + \hat{\omega})^2 - 1\}, \end{aligned} \quad (179)$$

where  $\hat{p}$  is now regarded as a function of  $E$  and  $\theta$ ,

$$\hat{p} = \pm \sqrt{2[E - \hat{\phi}(\theta)]}. \quad (180)$$

Equation (179) is exact, but an exact nontrivial solution cannot be found analytically. Here we expand the solution in powers of  $\hat{\nu}$ , writing

$$\mathbf{h} = \mathbf{h}_0 + \hat{v}\mathbf{h}_1 + \dots \quad (181)$$

Then to lowest order in  $\hat{v}$ , Eq. (179) is simply

$$\left. \frac{\partial \mathbf{h}_0}{\partial \theta} \right|_E = 0, \quad (182)$$

with the solution  $\mathbf{h}_0 = \mathbf{h}_0(E)$ . The functional form of  $\mathbf{h}_0$  is determined by the next-order equation,

$$\begin{aligned} \hat{p} \left. \frac{\partial \mathbf{h}_1}{\partial \theta} \right|_E = & \hat{p} \left[ \frac{\partial}{\partial E} \left( \hat{p} \frac{\partial \mathbf{h}_0}{\partial E} \right) + (2\hat{\alpha} - \hat{\omega} - \hat{p}) \frac{\partial \mathbf{h}_0}{\partial E} \right. \\ & \left. + \hat{\alpha} \left( \frac{\hat{\alpha} - \hat{\omega}}{\hat{p}} - 1 \right) \mathbf{h}_0 \right] \\ & - \frac{e^{-\hat{\alpha}\hat{p}}}{\hat{\alpha}} \{0, m\bar{v}(\hat{p} + \hat{\omega}), (\hat{p} + \hat{\omega})^2 - 1\}. \end{aligned} \quad (183)$$

For untrapped particles with energy  $E > \hat{\varepsilon}$ , we integrate Eq. (183) from  $\theta = 0$  to  $\theta = 2\pi$ . The boundary condition that  $\mathbf{h}_1(\theta = 0, E) = \mathbf{h}_1(\theta = 2\pi, E)$  then yields the following differential equation for  $\mathbf{h}_0(E)$ :

$$\begin{aligned} 0 = & \frac{\partial}{\partial E} \left( I \frac{\partial \mathbf{h}_0}{\partial E} \right) + (2\hat{\alpha} - \hat{\omega} - I) \frac{\partial \mathbf{h}_0}{\partial E} \\ & + \hat{\alpha} [(\hat{\alpha} - \hat{\omega})\tau - 1] \mathbf{h}_0 + \mathbf{z}(E), \quad E > \hat{\varepsilon}, \end{aligned} \quad (184)$$

where

$$\mathbf{z}(E) = -\frac{1}{\hat{\alpha}} \int_0^{2\pi} \frac{d\theta}{2\pi} \frac{e^{-\hat{\alpha}\hat{p}}}{\hat{p}} \{0, m\bar{v}(\hat{p} + \hat{\omega}), (\hat{p} + \hat{\omega})^2 - 1\} \quad (185)$$

and  $I(E)$  and  $\tau(E)$  are the action and period per radian, respectively, of the untrapped motion,

$$I(E) = \int_0^{2\pi} \frac{d\theta}{2\pi} \hat{p}(E, \theta), \quad (186)$$

$$\tau(E) = \frac{\partial I}{\partial E} = \int_0^{2\pi} \frac{d\theta}{2\pi \hat{p}(E, \theta)}. \quad (187)$$

Note that  $I$  and  $\tau$  are positive for  $\hat{p} > 0$  and negative for  $\hat{p} < 0$ . The corresponding solutions to Eq. (184) will be called  $\mathbf{h}_0^+$  and  $\mathbf{h}_0^-$ , respectively.

For trapped particles with energy  $-\hat{\varepsilon} \leq E \leq \hat{\varepsilon}$ , we perform an integral in  $\theta$  over a cycle of the trapped particle orbit. The condition that  $\mathbf{h}_1$  is a single-valued function of  $\theta$  leads to the following equation for  $\mathbf{h}_0$ :

$$0 = \frac{\partial}{\partial E} \left( I_t \frac{\partial \mathbf{h}_0}{\partial E} \right) - I_t \frac{\partial \mathbf{h}_0}{\partial E} + \hat{\alpha}(\hat{\alpha} - \hat{\omega})\tau_t \mathbf{h}_0 + \mathbf{z}_t, \quad |E| \leq \hat{\varepsilon}, \quad (188)$$

where

$$\mathbf{z}_t = -\frac{1}{\hat{\alpha}} \oint \frac{d\theta}{2\pi} \frac{e^{-\hat{\alpha}\hat{p}}}{\hat{p}} \{0, m\bar{v}(\hat{p} + \hat{\omega}), (\hat{p} + \hat{\omega})^2 - 1\} \quad (189)$$

and  $I_t$  and  $\tau_t$  are the action and period per radian, respectively, of the trapped motion,

$$I_t = \oint \frac{d\theta}{2\pi} \hat{p}, \quad (190)$$

$$\tau_t = \frac{\partial I_t}{\partial E} = \oint \frac{d\theta}{2\pi \hat{p}}. \quad (191)$$

In Eqs. (189)–(191), the integral  $\oint d\theta$  denotes an integration over a single orbital cycle of the trapped motion, holding energy  $E$  fixed.

Equations (184) and (188) are second-order inhomogeneous ordinary differential equations (ODEs) for  $\mathbf{h}_0(E)$ . We will solve these ODEs using the method of variation of parameters, which requires knowledge of the homogeneous solutions to the ODEs.

We first consider the homogeneous solutions of the untrapped ODE, Eq. (184). In the range  $E \gg \hat{\varepsilon}$ ,

$$I(E) \simeq \pm \sqrt{2E}, \quad \tau(E) \simeq \pm 1/\sqrt{2E}, \quad E \gg \hat{\varepsilon}, \quad (192)$$

when the  $\pm$  signs refer to untrapped particles with  $\hat{p}$  greater or less than zero, respectively.

In this range the homogeneous solutions,  $v_1(E)$  and  $v_2(E)$ , are

$$\begin{aligned} v_1(E) = & e^{\mp \hat{\alpha}\sqrt{2E}} (1 + \sqrt{\pi/2} \hat{\alpha} e^{-\hat{\omega}^2/2} [\operatorname{erfi}(\pm \sqrt{E} + \hat{\omega}/\sqrt{2}) \\ & - \operatorname{erfi}(\hat{\omega}/\sqrt{2})]), \quad E \gg \hat{\varepsilon}, \end{aligned} \quad (193)$$

$$v_2(E) = e^{\mp \hat{\alpha}\sqrt{2E}}, \quad E \gg \hat{\varepsilon}, \quad (194)$$

where  $\operatorname{erfi}(x) = 2/\sqrt{\pi} \int_0^x e^{z^2} dz$  is the error function with an imaginary argument.

Furthermore, we can show that the homogeneous solutions are finite at  $E = \hat{\varepsilon}$ , with finite first derivatives. Noting that  $I = O(\sqrt{\hat{\varepsilon}})$  as  $E \rightarrow \hat{\varepsilon}$ , and  $\tau = O(1/\sqrt{\hat{\varepsilon}})$ , with an integrable singularity as  $E \rightarrow \hat{\varepsilon}$ , we solve Eq. (184) in the asymptotic limit  $E \ll 1$  for the two homogeneous solutions. These satisfy the following dominant balances in the ODE:

$$\frac{\partial}{\partial E} \left( I \frac{\partial v_2}{\partial E} \right) = 0, \quad E \ll 1 \quad (195)$$

and

$$\tau \left[ \frac{\partial v_1}{\partial E} + \hat{\alpha}(\hat{\alpha} - \hat{\omega})v_1 \right] = 0, \quad E \ll 1. \quad (196)$$

The general solution to Eq. (195),

$$v_2 = C_1 + C_2 \int_{\hat{\varepsilon}}^E \frac{dE}{I} \quad (197)$$

can be matched to the outer solution for  $v_2$ , given by Eq. (194). To lowest order in  $\varepsilon$ , the matching conditions on the function and its first derivative require  $C_1 = 1$  and  $C_2 = -\hat{\alpha}$ . Thus,

$$v_2 = 1 - \hat{\alpha} \int_{\hat{\varepsilon}}^E \frac{dE}{I} + O(E), \quad E \ll 1. \quad (198)$$

The solution to Eq. (196),

$$v_1 = C_1 e^{-\hat{\alpha}(\hat{\alpha}-\hat{\omega})E}, \quad E \ll 1 \quad (199)$$

can be matched to the outer solution, Eq. (193), by taking  $C_1=1$ . Thus

$$v_1 = 1 - \hat{\alpha}(\hat{\alpha} - \hat{\omega})E + O(E^{3/2}), \quad E \ll 1. \quad (200)$$

The inhomogeneous solution to Eq. (184) can be constructed from  $v_1$  and  $v_2$ ,

$$\begin{aligned} \mathbf{h}_0(E) = v_2(E) \int_{\hat{\varepsilon}}^E dE' \frac{v_1(E') \mathbf{z}(E')}{I(E') W(E')} \\ - v_1(E) \int_{\infty}^E dE' \frac{v_2(E') \mathbf{z}(E')}{I(E') W(E')} + \boldsymbol{\beta}_1 v_2(E), \quad E > \hat{\varepsilon}, \end{aligned} \quad (201)$$

where  $\boldsymbol{\beta}_1$  is a vector of undetermined coefficients and the Wronskian  $W$  is defined as

$$W(E) = v_1' v_2 - v_2' v_1. \quad (202)$$

The integration limit on the second integral is chosen so that inner products involving  $h_0$  are finite (since as  $E \rightarrow \infty$ ,  $v_1 \rightarrow \infty$  like  $e^E$ ).

In the regime  $E \gg \varepsilon$ , the solution for  $h_0$  can be found by using Eqs. (192) and (194), along with

$$\begin{aligned} \mathbf{z}(E) = \mp \frac{e^{\mp \hat{\alpha} \sqrt{2E}}}{\hat{\alpha} \sqrt{2E}} \{0, m\bar{v}(\hat{\omega} \pm \sqrt{2E}), (\hat{\omega} \pm \sqrt{2E})^2 - 1\}, \\ E \gg \varepsilon. \end{aligned} \quad (203)$$

To lowest order in  $\varepsilon$ , the integration limit on the first integral in Eq. (201) can be changed from  $\hat{\varepsilon}$  to zero. The integrations then yield

$$\begin{aligned} \mathbf{h}_0 = - \frac{e^{\mp \hat{\alpha} \sqrt{2E}}}{\hat{\alpha}^2} \{0, m\bar{v}(1 \pm \hat{\alpha} \sqrt{2E}), \hat{\omega} + \hat{\alpha}(E \pm \hat{\omega} \sqrt{2E})\} \\ + \boldsymbol{\beta}_1 e^{\mp \hat{\alpha} \sqrt{2E}}, \quad E \gg \hat{\varepsilon}. \end{aligned} \quad (204)$$

Turning now to the solution for  $\mathbf{h}_0$  in the trapping region  $-\hat{\varepsilon} \leq E \leq \hat{\varepsilon}$ , we consider the homogeneous solutions to Eq. (188),  $v_{r1}(E)$  and  $v_{r2}(E)$ . Just as for the untrapped solution when  $E \ll 1$ , there are two consistent dominant balances in Eq. (188) that describe the two homogeneous solutions,

$$\frac{d}{dE} \left( I_t \frac{dv_{r1}}{dE} \right) = O\left( \frac{1}{\sqrt{\hat{\varepsilon}}} \right), \quad (205)$$

$$\frac{d}{dE} v_{r2} + \hat{\alpha}(\hat{\alpha} - \hat{\omega})v_{r2} = O(\hat{\varepsilon}). \quad (206)$$

Equation (205) has the general solution

$$v_{r1} = C_1 + C_2 \int_{\hat{\varepsilon}}^E \frac{dE}{I_t} + O(\hat{\varepsilon}^{3/2}). \quad (207)$$

Since  $I_t \rightarrow (E + \hat{\varepsilon})/\omega_t$  as  $E \rightarrow -\hat{\varepsilon}$ , where  $\omega_t = \sqrt{\varepsilon}$  is the frequency of harmonic oscillations,  $v_{r1}$  is logarithmically divergent as  $E \rightarrow -\hat{\varepsilon}$ .

Equation (206) has the solution

$$v_{r2} = e^{-\hat{\alpha}(\hat{\alpha}-\hat{\omega})(E-\hat{\varepsilon})} + O(\hat{\varepsilon}^2). \quad (208)$$

The trapped solution for  $\mathbf{h}_0$  can be constructed from  $v_{r1}$  and  $v_{r2}$ ,

$$\begin{aligned} \mathbf{h}_0(E) = v_{r2}(E) \int_{+\hat{\varepsilon}}^E \frac{dE' v_{r1}(E') \mathbf{z}_t(E')}{I_t(E') W_t(E')} \\ - v_{r1}(E) \int_{-\hat{\varepsilon}}^E \frac{dE' v_{r2}(E') \mathbf{z}_t(E')}{I_t(E') W_t(E')} + \boldsymbol{\beta}_2 v_{r2}(E), \quad |E| \leq \hat{\varepsilon}, \end{aligned} \quad (209)$$

where  $W_t = v_{r1}' v_{r2} - v_{r2}' v_{r1}$ , and  $\boldsymbol{\beta}_2$  is a vector of undetermined coefficients. A continuous solution for  $\mathbf{h}_0$  across the separatrix can be found by choosing  $\boldsymbol{\beta}_1$  and  $\boldsymbol{\beta}_2$  appropriately. Matching the inner and outer values of  $h_0$  at  $E = \hat{\varepsilon}$  yields

$$\begin{aligned} \boldsymbol{\beta}_1 + v_{r1}(\hat{\varepsilon}) \int_{\hat{\varepsilon}}^{\infty} \frac{dE' v_2(E') \mathbf{z}(E')}{I(E') W(E')} \\ = \boldsymbol{\beta}_2 - v_{r1}(\hat{\varepsilon}) \int_{-\hat{\varepsilon}}^{\hat{\varepsilon}} \frac{dE' v_{r2}(E') \mathbf{z}_t(E')}{I_t(E') W_t(E')}. \end{aligned} \quad (210)$$

The integral on the right-hand side yields a result of  $O(\sqrt{\hat{\varepsilon}})$ . The integral on the left-hand side can be determined approximately by using the  $E \gg \hat{\varepsilon}$  forms of  $I$ ,  $v_1$ ,  $v_2$ , and  $\mathbf{z}$  from Eqs. (192)–(194) and (203). The result of the integration yields

$$\boldsymbol{\beta}_1 - \frac{1}{\hat{\alpha}^2} (0, m\bar{v}, \hat{\omega}) = \boldsymbol{\beta}_2 + O(\sqrt{\hat{\varepsilon}}). \quad (211)$$

Although  $\mathbf{h}_0(E)$  is continuous across the separatrix,  $\partial \mathbf{h}_0 / \partial E$  is not. The jump in the first derivative is given by subtracting the derivatives of Eqs. (201) and (209),

$$\begin{aligned} \frac{\partial \mathbf{h}_0(\hat{\varepsilon}^+)}{\partial E} - \frac{\partial \mathbf{h}_0(\hat{\varepsilon}^-)}{\partial E} = - \frac{\hat{\alpha} \boldsymbol{\beta}_1}{I(\hat{\varepsilon})} - \hat{\alpha}(\hat{\alpha} - \hat{\omega}) \int_{\infty}^{\hat{\varepsilon}} dE' \frac{v_2(E') \mathbf{z}(E')}{I(E') W(E')} \\ + \boldsymbol{\beta}_2 \hat{\alpha}(\hat{\alpha} - \hat{\omega}) \\ + \frac{\partial}{\partial E} v_{r1}(\hat{\varepsilon}) \int_{-\hat{\varepsilon}}^{\hat{\varepsilon}} dE' \frac{v_{r2}(E') \mathbf{z}_t(E')}{I_t(E') W_t(E')}. \end{aligned} \quad (212)$$

The integral from  $-\hat{\varepsilon} < E < \hat{\varepsilon}$  is of the order  $\sqrt{\hat{\varepsilon}}$ , while the integral from  $\hat{\varepsilon} < E < \infty$  is of order unity. Therefore, we can neglect the integrals to lowest order in  $\hat{\varepsilon}$ , obtaining

$$\frac{\partial \mathbf{h}_0(\hat{\varepsilon}^+)}{\partial E} - \frac{\partial \mathbf{h}_0(\hat{\varepsilon}^-)}{\partial E} = - \frac{\hat{\alpha} \boldsymbol{\beta}_1}{I(\hat{\varepsilon})} + O(1). \quad (213)$$

Finally,  $\boldsymbol{\beta}_1$  is determined via the constraint condition  $(1, \mathbf{g})_{p_\theta} = 0$ . To lowest order in  $\hat{\varepsilon}$  and  $\nu$  the trapping region can be neglected in this inner product, and the  $E \gg \hat{\varepsilon}$  form of  $\mathbf{h}_0$ , given by Eq. (204), can be substituted for  $\mathbf{h}$ ,

$$0 = (1, \mathbf{g}) \cong \frac{N}{\sqrt{2\pi m T}} \int d\theta dz dp_z e^{(p_z^2/2m - mV_b^2/2)/T_b} \times \left\{ \frac{T_b}{\alpha}, \frac{T_b}{\alpha} \left( p_z'' + \frac{kT_b}{\ell\alpha} \right), \frac{1}{\alpha} \left( \frac{p_z''^2}{2m} - \frac{T_b}{2} \right) + \frac{T_b \omega_0}{\alpha^2} \right\} + \left[ \boldsymbol{\beta}_1 - \frac{1}{\hat{\alpha}^2} \{ 0, m\bar{v}(1 + \hat{\alpha}\hat{p}), \hat{\omega} + \hat{\alpha}(\hat{p}^2/2 + \hat{\omega}\hat{p}) \} \right] \frac{\ell m \bar{v}}{k}, \quad (214)$$

where  $p_z'' = m\bar{v}(\hat{p} + \hat{\omega})$  and  $E \cong \hat{p}^2/2$ . After performing the integrations we obtain

$$\boldsymbol{\beta}_1 = -\frac{1}{\hat{\alpha}} \left\{ 1, m\bar{v}\hat{\omega}, \frac{\hat{\omega}^2 - 1}{2} \right\}. \quad (215)$$

We now use these results to evaluate the transport coefficients  $\mu_{ij}$ . Since  $(1, g_i)_{p_\theta} = 0$ , Eq. (131) implies

$$\mu_{ij} = \frac{1}{T_b} (s_i, g_j)_{p_\theta}. \quad (216)$$

The required inner product, written in terms of  $h_j$  using Eqs. (174) and (176), is

$$(s, g_j)_{p_\theta} = \frac{\ell m \bar{v} T_b \bar{n} e^{-\hat{\omega}^2/2}}{(2\pi)^{3/2} k} \int d\theta d\hat{p} e^{-E + (\hat{\alpha} - \hat{\omega})\hat{p}} h_j \frac{\partial \hat{\phi}}{\partial \theta} \times \left\{ 1, m\bar{v}(\hat{\omega} + \hat{p}), E + \hat{\omega}\hat{p} + \frac{\hat{\omega}^2 - 1}{2} - \bar{\phi}/T_b \right\}. \quad (217)$$

We have also substituted for  $\mathbf{s}$  using Eq. (125), in terms of scaled variables. The integrals may be manipulated into a more useful form by first converting the  $\hat{p}$  integral to one over energy, noting that  $d\hat{p} = dE/|\hat{p}|(E, \theta)$  and  $\partial|\hat{p}|/\partial\theta = -\partial\hat{\phi}/\partial\theta/|\hat{p}|$ ,

$$(s, g_j)_{p_\theta} = -\frac{\ell m \bar{v} T_b \bar{n} e^{-\hat{\omega}^2/2}}{(2\pi)^{3/2} k} \int d\theta dE e^{-E} \frac{\partial|\hat{p}|}{\partial\theta} \left[ h_j^+ e^{(\hat{\alpha} - \hat{\omega})|\hat{p}|} \times \left\{ 1, m\bar{v}(\hat{\omega} + |\hat{p}|), E + \hat{\omega}|\hat{p}| + \frac{\hat{\omega}^2 - 1}{2} - \frac{\bar{\phi}}{T_b} \right\} + h_j^- e^{-(\hat{\alpha} - \hat{\omega})|\hat{p}|} \left\{ 1, m\bar{v}(\hat{\omega} - |\hat{p}|), E - \hat{\omega}|\hat{p}| + \frac{\hat{\omega}^2 - 1}{\hat{p}} - \frac{\bar{\phi}}{T_b} \right\} \right]. \quad (218)$$

Here,  $h_j^+$  and  $h_j^-$  refer to solutions for  $h_j$  at positive and negative  $\hat{p}$ , respectively. It is possible to integrate this expression by parts in  $\theta$ ,

$$(s, g_j)_{p_\theta} = \frac{\ell m \bar{v} T_b \bar{n} e^{-\hat{\omega}^2/2}}{(2\pi)^{3/2} k} \int d\theta dE e^{-E} \frac{|\hat{p}|}{\hat{\alpha} - \hat{\omega}} \left[ \frac{\partial h_j^+}{\partial \theta} e^{(\hat{\alpha} - \hat{\omega})|\hat{p}|} \times \left\{ 1, m\bar{v} \left( \hat{\omega} - \frac{1}{\hat{\alpha} - \hat{\omega}} + |\hat{p}| \right), E + \hat{\omega}|\hat{p}| - \frac{\hat{\omega}}{\hat{\alpha} - \hat{\omega}} + \frac{\hat{\omega}^2 - 1}{2} - \frac{\bar{\phi}}{T_b} \right\} - \frac{\partial h_j^-}{\partial \theta} e^{-(\hat{\alpha} - \hat{\omega})|\hat{p}|} \times \left\{ 1, m\bar{v} \left( \hat{\omega} - \frac{1}{\hat{\alpha} - \hat{\omega}} - |\hat{p}| \right), E - \hat{\omega}|\hat{p}| - \frac{\hat{\omega}}{\hat{\alpha} - \hat{\omega}} + \frac{\hat{\omega}^2 - 1}{2} - \frac{\bar{\phi}}{T_b} \right\} \right]. \quad (219)$$

The derivatives  $\partial h_j^+/\partial\theta$  and  $\partial h_j^-/\partial\theta$  are given in perturbation theory by Eqs. (181) and (183). For  $E \gg \hat{\varepsilon}$ , where  $\hat{p} \rightarrow \pm\sqrt{2E}$ , Eqs. (183), (184), and (193) imply that  $\partial h_i^\pm/\partial\theta \rightarrow 0$ . Therefore, we only require  $\partial h_i/\partial\theta$  for  $E \sim O(\hat{\varepsilon})$ , which implies  $|\hat{p}| \sim O(\sqrt{\hat{\varepsilon}}) \ll 1$ . We may then Taylor expand the exponential to first order,

$$e^{\pm(\hat{\alpha} - \hat{\omega})|\hat{p}|} \approx 1 \pm (\hat{\alpha} - \hat{\omega})|\hat{p}|. \quad (220)$$

Noting that  $\int_0^{2\pi} d\theta \partial h_j^\pm/\partial\theta = 0$  for untrapped particles, and  $\oint d\theta \partial h_j/\partial\theta = \int d\theta (\partial h_j^+/\partial\theta - \partial h_j^-/\partial\theta) = 0$  for trapped particles, many terms cancel. Keeping other terms only to lowest order in  $\hat{\varepsilon}$  yields the simple expression

$$(s, g_j)_{p_\theta} = \frac{\ell m \bar{v} T_b \bar{n} e^{-\hat{\omega}^2/2}}{(2\pi)^{3/2} k} \hat{\boldsymbol{\beta}} \int d\theta dE |\hat{p}| \left( \frac{\partial h_j^+}{\partial \theta} + \frac{\partial h_j^-}{\partial \theta} \right), \quad (221)$$

where

$$\hat{\boldsymbol{\beta}} = \left\{ 1, m\bar{v}\hat{\omega}, \frac{\hat{\omega}^2 - 1}{2} \right\}. \quad (222)$$

Substituting Eqs. (181) and (183) for  $\partial h_i^\pm/\partial\theta$ , we obtain three contributions to the integral: from the trapped region, the untrapped region, and the jump in  $\partial h_j/\partial E$  at the separatrix. Only the latter two contributions are important when  $\hat{\varepsilon} \ll 1$ , so we will not further consider the trapped contribution. Then the transport coefficient  $\mu_{ij}$  is, to lowest order in  $\hat{\varepsilon}$ , given by

$$\mu_{ij} = \frac{\ell m \bar{v} \bar{n} e^{-\hat{\omega}^2/2}}{\sqrt{\pi} k} \hat{\boldsymbol{\beta}}_i \hat{v} \left( 2\hat{\varepsilon} \left[ \frac{\partial h_{0j}^+(\hat{\varepsilon}^+)}{\partial E} - \frac{\partial h_{0j}^+(\hat{\varepsilon}^-)}{\partial E} - \frac{\partial h_{0j}^-(\hat{\varepsilon}^+)}{\partial E} + \frac{\partial h_{0j}^-(\hat{\varepsilon}^-)}{\partial E} \right] + \int_{\hat{\varepsilon}}^{\infty} dE \left\{ 2E \frac{\partial^2 h_{0j}^+}{\partial E^2} + [(2\hat{\alpha} - \hat{\omega})|I| - 2E + 1] \frac{\partial h_{0j}^+}{\partial E} + \hat{\alpha}(\hat{\omega} - \hat{\alpha} - |I|) h_{0j}^+ - 2E \frac{\partial^2 h_{0j}^-}{\partial E^2} + [(2\hat{\alpha} - \hat{\omega})|I| + 2E - 1] \frac{\partial h_{0j}^-}{\partial E} + \hat{\alpha}(\hat{\alpha} - \hat{\omega} - |I|) h_{0j}^- \right\} \right). \quad (223)$$

Here we have used the fact that the inhomogeneous terms in Eq. (183) for  $\hat{p} > 0$  and  $\hat{p} < 0$  cancel to lowest order in  $\hat{\varepsilon}$ . The jump in the first derivative of  $h_{0j}$  across the separatrix is given by Eq. (213). We next simplify the integral by substituting for  $\partial^2 h_{0j}^{\pm} / \partial E^2$  using Eq. (184),

$$\begin{aligned} \mu_{ij} = & \frac{\ell m \bar{\nu} \bar{n} e^{-\hat{\omega}^2/2}}{\sqrt{2\pi k}} \hat{\beta}_i \hat{\nu} \left( -4 \hat{\alpha} \beta_{1j} \frac{\hat{\varepsilon}}{|I(\hat{\varepsilon})|} \right. \\ & + \int_{\varepsilon}^{\infty} dE \left\{ \left( |I| - \frac{2E}{|I|} \right) \left[ (2\hat{\alpha} - \hat{\omega}) \left( \frac{\partial h_{0i}^+}{\partial E} + \frac{\partial h_{0i}^-}{\partial E} \right) \right. \right. \\ & \left. \left. - \hat{\alpha} (h_{0j}^+ + h_{0j}^-) \right] + \left( 1 - \frac{2E|\tau|}{|I|} \right) \right. \\ & \left. \times \left[ \frac{\partial h_{0i}^+}{\partial E} - \frac{\partial h_{0i}^-}{\partial E} + \hat{\alpha} (\hat{\alpha} - \hat{\omega}) (h_{0j}^+ - h_{0j}^-) \right] \right\} \right). \quad (224) \end{aligned}$$

The functions  $|I| - 2E/|I|$  and  $1 - 2E|\tau|/|I|$  are nonzero only for  $E \sim \hat{\varepsilon}$ , so  $E \ll 1$  forms of  $h_{0j}$  and  $\partial h_{0j} / \partial E$  may be employed. Furthermore, it is easily seen that

$$\int_{\hat{\varepsilon}}^{\infty} dE \left( |I| - \frac{2E}{|I|} \right) = O(\hat{\varepsilon}^{3/2}) \quad (225)$$

and

$$\int_{\hat{\varepsilon}}^{\infty} dE \left( 1 - \frac{2E|\tau|}{|I|} \right) = O(\hat{\varepsilon}). \quad (226)$$

This implies that, to lowest order in  $\hat{\varepsilon}$ , only the term in the integral involving  $\partial h_{0j}^+ / \partial E - \partial h_{0j}^- / \partial E$  need be kept. Furthermore, these derivatives may be replaced to lowest order by  $\beta_{1j} \partial \nu_{2j}^+ / \partial E$ , since the other terms in Eq. (201) yield a comparatively negligible contribution. Using Eq. (198) to determine  $\partial \nu_{2j} / \partial E$  near  $E = \hat{\varepsilon}$  then yields

$$\begin{aligned} \mu_{ij} = & \frac{\ell m \bar{\nu} \bar{n} e^{-\hat{\omega}^2/2}}{\sqrt{2\pi k}} \hat{\beta}_i \hat{\nu} \left[ -4 \hat{\alpha} \beta_{1j} \frac{\hat{\varepsilon}}{|I(\hat{\varepsilon})|} \right. \\ & \left. - 2 \hat{\alpha} \beta_{1j} \int_{\hat{\varepsilon}}^{\infty} \frac{dE}{|I|} \left( 1 - \frac{2E|\tau|}{|I|} \right) \right]. \quad (227) \end{aligned}$$

Using Eq. (215) for  $\beta_{1j}$ , the remaining dependence on  $\hat{\alpha}$  cancels and we are left with the following simple asymptotic expression for transport coefficients in the banana regime:

$$\mu_{ij} = \sqrt{\frac{2}{\pi}} \frac{\ell m \bar{\nu} \bar{n}}{k} \hat{\nu} e^{-\hat{\omega}^2/2} \hat{\beta}_i \hat{\beta}_j \left[ \frac{2\hat{\varepsilon}}{|I(\hat{\varepsilon})|} + \int_{\hat{\varepsilon}}^{\infty} \frac{dE}{|I|} \left( 1 - \frac{2E|\tau|}{|I|} \right) \right]. \quad (228)$$

For the Hamiltonian of Eq. (141),  $|I(\hat{\varepsilon})| = 4\sqrt{\hat{\varepsilon}}/\pi$ , and

$$\int_{\hat{\varepsilon}}^{\infty} \frac{dE}{|I|} \left( 1 - \frac{2E|\tau|}{|I|} \right) = -0.0192\sqrt{\hat{\varepsilon}}. \quad (229)$$

This implies that

$$\mu_{ij} = 1.100 \frac{\ell m \bar{\nu} \bar{n}}{k} \hat{\nu} e^{-\hat{\omega}^2/2} \sqrt{\hat{\varepsilon}} \hat{\beta}_i \hat{\beta}_j. \quad (230)$$

This result shows that the form of the transport coefficient matrix given by Eq. (161) for the linear regime still holds in the banana regime. The scaling of Eq. (230) agrees with Eq. (3).

We have compared Eq. (230) to numerical calculations of the transport coefficients in the banana regime, obtained by solving Eqs. (127) and (128) for  $g_i$  and  $G_1$ , respectively. The numerical approach employed is to solve the generic equation

$$\hat{L}_{\ell} g = s(\theta, p_z'') \quad (231)$$

by expanding  $g$  in Hermite polynomials and Fourier modes,

$$g = \sum_{n=0}^N \sum_{j=-J}^J \tilde{g}_{jn} H_n \left( \frac{p_z''}{\sqrt{2mT_b}} \right) e^{ij\theta}. \quad (232)$$

Equation (231) then implies

$$\sum_{\bar{j}\bar{n}} L_{jn\bar{j}\bar{n}} g_{\bar{j}\bar{n}} = s_{jn}, \quad (233)$$

where

$$s_{jn} = \int d\theta dz dp_z'' f_{00} e^{-ij\theta} H_n e^{-p_z''^2/2mT_b} s \quad (234)$$

and

$$L_{jn\bar{j}\bar{n}} = \int d\theta dz dp_z'' f_{00} e^{-ij\theta} H_n e^{-p_z''^2/2mT_b} \hat{L}_{\ell} (e^{ij\theta} H_{\bar{n}}). \quad (235)$$

The matrix  $L_{jn\bar{j}\bar{n}}$  is sparse, allowing relatively rapid solution of the linear equations for  $N$  up to 2000 and  $J$  up to 20. For small  $\varepsilon$  and small  $\nu$ , many terms must be kept in order to properly represent  $g$  across the narrow trapping region.

By solving Eqs. (127) and (128) using this numerical method, and using these results in Eq. (131), numerical values for  $\mu_{ij}$  are obtained and compared in Fig. 2 to the asymptotic results in Eq. (230). Good agreement is obtained when  $\hat{\nu}$  is sufficiently small.

We also have compared  $\mu_{11}$  to simulations of particle transport in the banana regime, using the methods described in Sec. III. These results also are in reasonably good agreement with the theory, as seen in Fig. 2.

## B. Example 2: Axially confined plasma

In the second example of field error transport, the plasma is trapped in the  $z$ -direction by an external potential. The Hamiltonian is

$$H = \frac{p_z^2}{2m} - \omega_0 p_{\theta} + \phi_0(z) + \delta\phi(p_{\theta}, \theta, z), \quad (236)$$

where we choose an external confinement potential varying as  $\phi_0(z) = T_b(z/L)^8$ , giving a plasma of length roughly  $2L$ . Also, we assume an asymmetry varying as  $\delta\phi = \varepsilon \cos \theta \sin kz$ . In the numerical solutions we assume  $kL = 4.21$ . For this potential, the axial bounce frequency  $\omega_b$  is a function of parallel energy  $E = p_z^2/2m + \phi_0(z)$ , given by

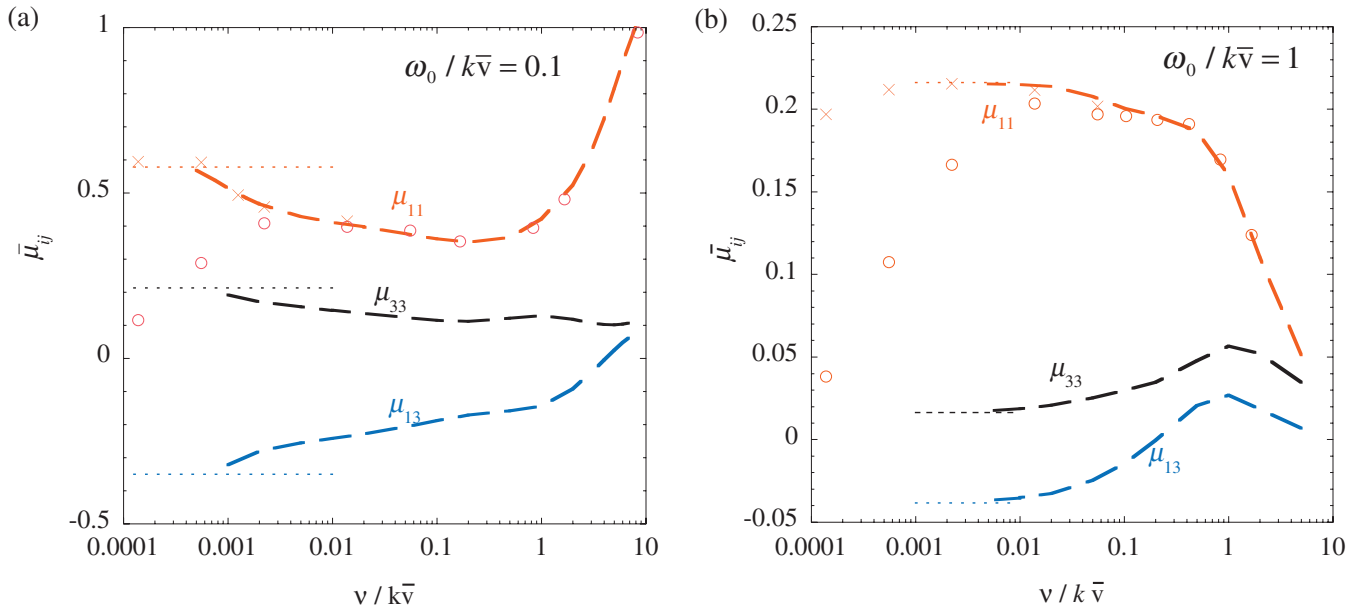


FIG. 3. (Color) The transport coefficients  $\mu_{11}$  (red),  $\mu_{13}$  (blue), and  $\mu_{33}$  (black) vs collision frequency  $\nu$ , scaled according to Eq. (162), for  $\omega_0/k\bar{v}=0.1$  in (a) and  $\omega_0/k\bar{v}=1$  in (b), for the axially confined plasma of example 2. Thick dashed lines display the linear theory. Dotted lines give the plateau limit. Open circles are simulation measurements of  $\mu_{11}$  based on Eq. (137), for  $\varepsilon/T_b=0.02$ . Crosses are simulation results for  $\varepsilon/T_b=0.002$ .

$\omega_B(E)=0.453(E/T_b)^{3/8}k\bar{v}$ . The external potential ensures that  $\bar{V}=0$  in equilibrium.

As in example 1, we assume a nonconservative collision operator given by Eq. (117), and we further assume  $V_b=0$  for simplicity. The transport coefficients of interest then involve only particle and heat fluxes, i.e.,  $\mu_{11}$ ,  $\mu_{13}$ ,  $\mu_{31}$ , and  $\mu_{33}$ . We calculate these coefficients numerically via Eq. (131), after solving for the perturbed distribution using Eqs. (127) and (128). We also evaluate  $\mu_{11}$  using the particle simulation approach discussed in Sec. III.

In order to obtain numerical solutions for the transport coefficients, we expand the perturbed distribution function in the following basis functions:

$$g(\theta, z, p_z) = \sum_{j\ell n} g_{j\ell n} e^{i\ell\theta} \chi_j(z) H_n \left( \frac{p_z}{\sqrt{2mT_b}} \right), \quad (237)$$

where  $\chi_j(z)$  is an element from a complete set of  $z$  basis functions. We solve for  $g_{j\ell n}$  by substituting Eq. (237) into Eq. (127), yielding the matrix equation

$$\sum_{\bar{j}\ell\bar{n}} L_{j\ell n \bar{j}\ell\bar{n}} g_{\bar{j}\ell\bar{n}} = (\chi_j H_n e^{i\ell\theta}, s)_{p_\theta}, \quad (238)$$

where

$$L_{j\ell n \bar{j}\ell\bar{n}} = (\chi_j H_n e^{i\ell\theta}, \hat{L} \chi_{\bar{j}} H_{\bar{n}} e^{i\ell\theta})_{p_\theta}. \quad (239)$$

The basis functions  $\chi_j(z)$  are chosen as

$$\chi_j = e^{ijkz} \quad (240)$$

with  $j$  an integer in the range  $-M_z \leq j \leq M_z$ . A typical value of  $M_z$  might be up to several hundred in order to achieve good convergence for  $\mu_{ij}$ . We also sum over up to several hundred momentum basis functions. Since the total number of terms in the sums is rather large, we focus on the linear regime where we need keep only  $\ell = \pm 1$ .

Solutions for the transport coefficients in the linear regime are displayed in Fig. 3 for  $\omega_0/k\bar{v}=0.1$  and 1, as a function of  $\nu/k\bar{v}$ . These rotation frequencies correspond to rigidity  $R \equiv \omega_B(T_b)/\omega_0$  equal to 4.53 and 0.453, respectively (rigidity is a parameter used to characterize some experiments). Simulation results for  $\mu_{11}$  are also displayed in Fig. 3 and show agreement with the theory predictions except at low  $\nu/k\bar{v}$ , where banana trapping is becoming important, depending on the value of  $\varepsilon$ . As  $\varepsilon/T_b$  decreases, linear theory works at lower values of  $\nu/k\bar{v}$ , as expected from the scaling of the banana-plateau transition, Eq. (4). Qualitatively, these results mirror those of example 1.

### 1. Plateau regime

Transport coefficients in the plateau regime can be obtained analytically. In this regime we may replace the collision operator by a simple Krooks form, so that Eq. (127) becomes

$$-\omega_0 \frac{\partial g_j}{\partial \theta} + v_z \frac{\partial g_j}{\partial z} - \frac{\partial \phi_0}{\partial z} \frac{\partial g_j}{\partial p_z} + \nu g_j = s_j, \quad (241)$$

where  $\phi_0 = T_b(z/L)^8$  in our example. The equation can be solved using action angle variables  $(\psi, I)$  where

$$I = \oint p_z \frac{dz}{2\pi} \quad (242)$$

and  $\psi$  is the angle variable given, for  $v_z > 0$ , by

$$\psi = \int_0^z \frac{dz}{v_z} \omega_B(I), \quad (243)$$

where  $\omega_B = \partial E / \partial I$  is the axial bounce frequency.

In these variables, Eq. (241) becomes

$$-\omega_0 \frac{\partial g_j}{\partial \theta} + \omega_B \frac{\partial g_j}{\partial \psi} + \nu g_j = s_j. \quad (244)$$

Expanding  $g_j$  and  $s_j$  as Fourier series in  $\theta$  and  $\psi$ ,

$$g_j = \sum_{n,\ell} g_{jn\ell}(I) e^{in\psi + i\ell\theta}, \quad (245)$$

$$s_j = \sum_{n,\ell} s_{jn\ell}(I) e^{in\psi + i\ell\theta}, \quad (246)$$

the solution of Eq. (244) is

$$g_{jn\ell} = \frac{s_{jn\ell}}{in\omega_B(I) - i\ell\omega_0 + \nu}. \quad (247)$$

The transport coefficient  $\mu_{ij}$  is then

$$\begin{aligned} \mu_{ij} &= \frac{1}{T_b} \int d\theta dz dp_z f_{00} s_i g_j \\ &= \frac{2\pi}{T_b} \sum_{\ell} \int d\psi dI f_{00} \sum_{n,\bar{n}} g_{jn\ell} s_{i\bar{n}-\ell} e^{i(n-\bar{n})\psi} \\ &= \frac{(2\pi)^2}{T_b} \sum_{\ell n} \int dI f_{00} \frac{s_{jn\ell} s_{i\bar{n}-\ell}^*}{in\omega_B - i\ell\omega_0 + \nu}. \end{aligned} \quad (248)$$

Applying the Plemelj formula yields the plateau-regime transport coefficient

$$\mu_{ij} = \frac{4\pi^3}{T_b} \sum_{\ell n} \int dI s_{jn\ell} s_{i\bar{n}-\ell}^* f_{00} \delta[n\omega_B(I) - \ell\omega_0]. \quad (249)$$

Finally the Fourier coefficients  $s_{in\ell}$  are obtained using Eqs. (125) and (246),

$$\begin{aligned} \{s_{1n\ell}, s_{3n\ell}\} &= \int_0^{2\pi} \frac{d\psi}{2\pi} \int_0^{2\pi} \frac{d\theta}{2\pi} \frac{\partial \delta \phi}{\partial \theta} [p_\theta, \theta, z(I, \psi)] e^{-in\psi - i\ell\theta} \\ &\quad \times \left\{ 1, \frac{E - \bar{E}}{T_b} \right\}, \end{aligned} \quad (250)$$

where here  $\bar{E}$  is the mean parallel energy, equal to  $5T_b/8$  for the example potential, and  $z(I, \psi)$  is the axial position written in terms of action-angle variables via Eqs. (242) and (243).

Plots of the plateau regime values of  $\mu_{11}$ ,  $\mu_{13}$ , and  $\mu_{33}$  as a function of rotation frequency  $\omega_0$  are shown in Fig. 4. The plots display considerably more structure than the corresponding plots for example 1. The structure arises from the complex interplay between different bounce harmonics contributing to Eq. (249), and the results are sensitive to the precise form of the applied potentials.

Nevertheless, the transport coefficients still display the expected fluid, plateau, and banana regime behavior as collisionality decreases, as seen in Figs. 3(a) and 3(b). Note, however, that plateau regime values are not necessarily achieved before the banana regime takes over. As exemplified in Fig. 3(a), when  $\omega_0/k\bar{v} \ll 1$ , the linearized equations require  $\nu/k\bar{v} \ll 1$  before the plateau limiting values are attained. The banana regime can take over before this happens, depending on the value of  $\varepsilon/T$ . Thus, in realistic geometries with finite length plasmas for which  $\omega_0/k\bar{v} \ll 1$  (the regime

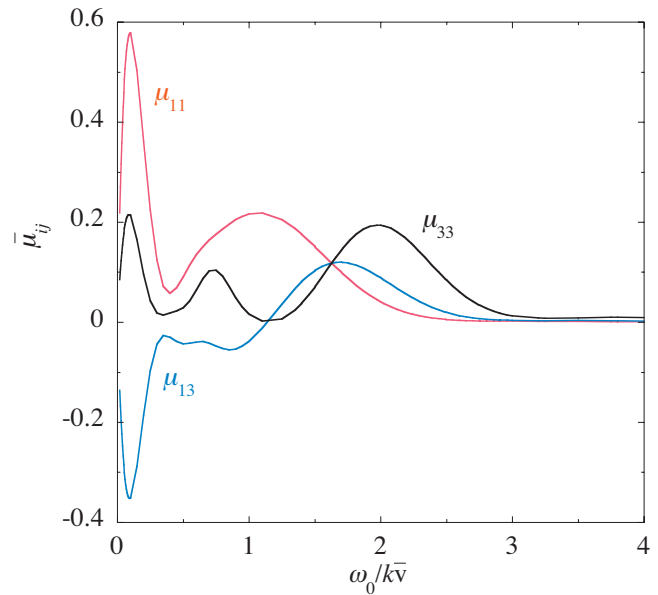


FIG. 4. (Color) Plateau limit of the transport coefficients for the model of example 2, scaled according to Eq. (162), and plotted vs rotation frequency.

of many experiments), plateau regime transport values may be of limited usefulness in predicting the transport. Rather, a full solution to the transport equation may be necessary, depending on the value of  $\varepsilon/T$  and  $\omega_0/k\bar{v}$ .

### C. Example 3: Added squeeze

In the final example, transport coefficients are calculated for an axially confined plasma to which a “squeeze” potential  $V_s$  is applied in the center. This generates a separatrix in the axial motion, with an x-point at  $z=0$ . The Hamiltonian is still given by Eq. (236), but now

$$\phi_0(z) = T_B(z/L)^8 + V_s e^{-50(kz)^4}. \quad (251)$$

Particles with energy less than  $V_s$  are trapped on either side of the squeeze potential and consequently experience only part of the field error, as opposed to particles with energy greater than  $V_s$  which move from end to end of the plasma. The different responses to the field error of the trapped and untrapped populations can lead to enhanced transport (here trapped and untrapped refer to trapping in the double well of  $\phi_0$ , not in the field error). This can be seen in Fig. 5 which plots the transport coefficient  $\mu_{11}$  versus  $\nu/k\bar{v}$ , obtained by solving Eq. (238) for  $V_s = T_b/2$ , using the same numerical method as described in example 2. When  $\omega_0 \geq k\bar{v}$ , the usual fluid, plateau and banana regimes are observed (not shown). However, when  $\omega_0$  falls well below  $k\bar{v}$ , two new transport regimes emerge: a  $1/\nu$  regime and a  $\sqrt{\nu}$  regime.

#### 1. $\omega_0 < \nu < k\bar{v}$ : The $1/\nu$ regime

Since the field error potential happens to be an odd function of  $z$ , low-energy particles trapped in the  $z < 0$  well of  $\phi_0$  experience the opposite field error potential from those trapped in the  $z > 0$  well. As a result, the  $\mathbf{E} \times \mathbf{B}$  drift orbits of particles in these two wells are displaced relative to one an-

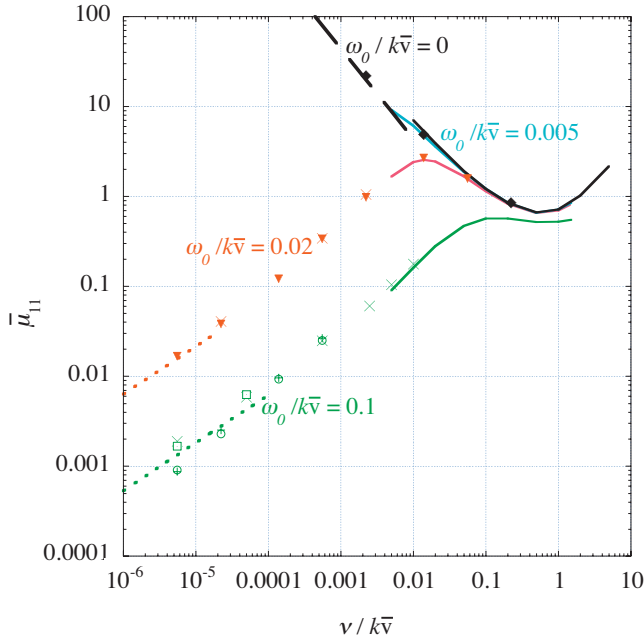


FIG. 5. (Color) The transport coefficient  $\mu_{11}$  for the model of example 3 with a squeeze potential  $V_s = 0.5T_b$ , scaled according to Eq. (162), and plotted vs collision frequency, for four different values of the rotation frequency:  $\omega_0 = 0$  (black),  $\omega_0/k\bar{v} = 0.005$  (blue),  $\omega_0/k\bar{v} = 0.02$  (red), and  $\omega_0/k\bar{v} = 0.1$  (green). Solid lines are linearized theory from Eqs. (156) and (237)–(240). The dashed line is the  $1/\nu$  regime limit of Eq. (260). The dotted lines are the  $\sqrt{\nu}$  regime limit of Eq. (268). The symbols display simulation results for  $\mu_{11}$  for a range of different  $\varepsilon$  values, from  $\varepsilon = 0.2$  to  $\varepsilon = 0.002$ .

other (see Fig. 6), and relative to untrapped particles. The magnitude  $\Delta r$  of the radial displacement is of order

$$\Delta r \sim \frac{\varepsilon}{m\Omega_c\omega_0 r}. \quad (252)$$

As particles wander in energy due to collisions they become detrapped and then retrapped on a time scale of order  $\nu^{-1}$ , assuming that  $V_s$  is of order  $T_b$ . Since particles only

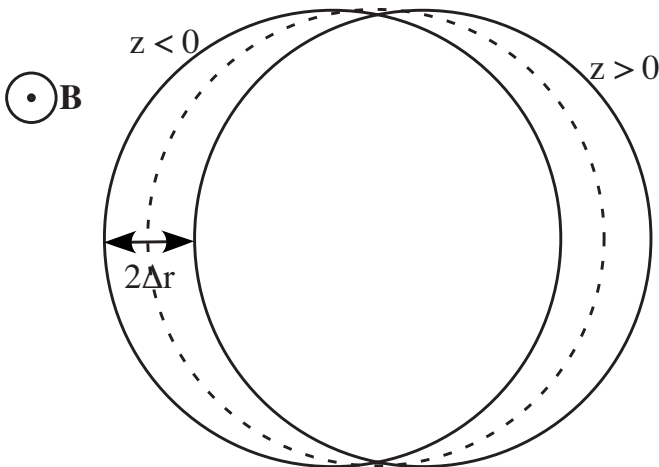


FIG. 6. Diagram of the effect of the field error on trapped and untrapped  $\mathbf{E} \times \mathbf{B}$  drift orbits. Trapped orbits are solid circles; the untrapped orbit is dotted.

complete a fraction of a drift orbit in this time, the magnitude of the radial drift step that they make is of order  $\Delta r\omega_0/\nu$ . The radial diffusion coefficient is then

$$D_r \sim \nu \left( \frac{\Delta r\omega_0}{\nu} \right)^2 \sim \frac{1}{\nu} \left( \frac{\varepsilon}{m\Omega_c r} \right)^2. \quad (253)$$

In the  $1/\nu$  regime, the particle diffusion increases as  $\nu$  decreases,<sup>2,32</sup> up to the point where  $\nu < \omega_0$ .

This estimate can be improved by solving Eq. (127) for  $g$ . A linear analysis suffices, in which case the equation becomes

$$v_z \frac{\partial \tilde{g}_{j\ell}}{\partial z} \Big|_E - i\ell\omega_0 \tilde{g}_{j\ell} - Dv_z \left( \frac{\partial}{\partial E} v_z \frac{\partial \tilde{g}_{j\ell}}{\partial E} - \frac{v_z}{T_b} \frac{\partial \tilde{g}_{j\ell}}{\partial E} \right) = \tilde{s}_{j\ell}, \quad (254)$$

where  $\tilde{s}_{j\ell}$  and  $\tilde{g}_{j\ell}$  are the  $\ell$ th Fourier components of  $s_j$  and  $g_j$  in  $\theta$ ,

$$E = \frac{p_z^2}{2m} + \phi_0(z) \quad (255)$$

is the zeroth-order parallel energy, and  $v_z = v_z(E, z)$  is the velocity at given energy  $E$ . Since we consider a regime where  $k\bar{v}$  is larger than either  $\nu$  or  $\omega_0$ , it is sensible to bounce-average Eq. (254) over  $z$  by acting on both sides with  $\oint dz / (2\pi v_z)$ , and focusing only on the bounce-averaged part of  $\tilde{g}_{j\ell}, \tilde{s}_{j\ell}$ . Replacing  $\tilde{g}_{j\ell}$  by  $\bar{g}_{j\ell}$  and carrying out the bounce-average yields

$$-i\ell\omega_0 \tau \bar{g}_{j\ell} - \nu T_b \left[ \frac{\partial}{\partial E} \left( I \frac{\partial \bar{g}_{j\ell}}{\partial E} \right) - \frac{I}{T_b} \frac{\partial \bar{g}_{j\ell}}{\partial E} \right] = \tau \bar{s}_{j\ell}, \quad (256)$$

where  $\bar{s}_{j\ell} = \tau^{-1} \oint \tilde{s}_{j\ell} dz / (2\pi v_z)$ ,  $I = \oint p_z dz / 2\pi$  is the action, and  $\tau = \oint dz / (2\pi v_z)$  is the period of the bounce motion modulo  $2\pi$ .

For energies  $E > V_s$ , the bounce-average of  $\bar{s}_{j\ell}$  is over the entire length of the plasma. Since  $\bar{s}_{j\ell}$  is odd in  $z$ ,  $\bar{s}_{j\ell} = 0$  in this energy range. The solution of Eq. (256) is simply  $\bar{g}_{j\ell} = 0$  for  $E > V_s$ . For trapped particles,  $\bar{g}_{j\ell} \neq 0$  since  $\bar{s}_{j\ell} \neq 0$ , taking opposite values in the two wells.

To make further analytic progress, we consider the limit  $\omega_0 \ll \nu$  and drop the first term in Eq. (256). A solution for  $\partial \bar{g}_{j\ell} / \partial E$  then follows immediately,

$$I \frac{\partial \bar{g}_{j\ell}}{\partial E} = C e^{E/T_b} - \int_0^E dE' \frac{\tau(E') \bar{s}_{j\ell}(E')}{\nu T_b} e^{(E-E')/T_b}, \quad (257)$$

where the constant  $C$  is determined by the condition that  $\bar{g}$  be finite as  $E \rightarrow 0$ . Since  $I(E) \rightarrow 0$  as  $E \rightarrow 0$ , this requires  $C = 0$ . Then the condition that  $\bar{g}_{j\ell}(V_s) = 0$  implies

$$\bar{g}_{j\ell} = \frac{1}{\nu T_b} \int_E^{V_s} \frac{dE''}{I(E'')} \int_0^{E''} dE' \tau(E') \bar{s}_{j\ell}(E') e^{(E''-E')/T_b}, \quad E \leq V_s. \quad (258)$$

Applying this result to the determination of the transport coefficients via Eq. (156) yields

$$\mu_{ij} = \frac{2\bar{n}}{T_b \int_{-\infty}^{\infty} dz e^{-\phi_0/T_b}} \sqrt{\frac{2\pi}{mT_b}} \times \sum_{\ell} \int_0^{V_s} dE e^{-E/T_b} \tau(E) \bar{g}_{j\ell}(E) \bar{s}_{i\ell}^*(E). \quad (259)$$

Here we substituted  $\bar{g}_j$  for  $g_j$ , made the variable change  $dz dp_z = dI d\psi = dE d\psi \tau(E)$ , and performed the  $\psi$  integral. An overall factor of 2 comes from the two trapping regions. Note the  $1/\nu$  dependence of the result, as expected from the estimate of Eq. (253). For the potential of Eq. (251), the energy integrals can be evaluated numerically, yielding, for  $V_s = T_b/2$ , and  $kL = 4.21$  (the parameters of Fig. 5),

$$\{\mu_{11}, \mu_{13}, \mu_{33}\} = \{0.0444, -0.0253, 0.0144\} \frac{\bar{n} \varepsilon^2}{\nu T_b}. \quad (260)$$

These asymptotic results match the numerical solution when  $\omega_0 \ll \nu \ll k\bar{v}$ , as seen in Fig. 5 for  $\mu_{11}$ .

More general results can be obtained for the case of long plasmas of length  $L$  with flat ends, for which  $I(E) \approx L\sqrt{2mE/\pi}$  and  $\tau(E) \approx L/(\sqrt{2E/m\pi})$ . Then the energy integrals in Eqs. (258) and (259) can be performed, and we can replace  $\int dz e^{-\phi_0/T_b} \approx L$ . The result for  $\mu_{ij}$  can be written as

$$\mu_{ij} = \frac{\bar{n}}{\nu T_b} \int \frac{d\theta}{2\pi} \left( \frac{\partial \bar{\delta}\phi}{\partial \theta} \right)^2 f_{ij}(V_s/T_b), \quad (261)$$

where  $\bar{\delta}\phi$  is the  $z$ -average of  $\delta\phi$  over the  $z > 0$  portion of the column, and the functions  $f_{ij}$  are defined as

$$f_{11}(x) = 2\sqrt{\pi} \int_0^{\sqrt{x}} dy e^{y^2} [\text{erf}(y)]^2, \quad (262)$$

$$f_{31}(x) = f_{13}(x) = \left( \frac{1}{2} - x \right) \text{erf}(\sqrt{x}) - \sqrt{\frac{x}{\pi}} e^{-x}, \quad (263)$$

and

$$f_{33}(x) = \frac{1}{2} \text{erf}(\sqrt{x}) - \sqrt{\frac{x}{\pi}} e^{-x}. \quad (264)$$

Here  $\text{erf}(x)$  is the error function.

An important feature of Eqs. (259) and (261) are their dependencies on the squeeze potential  $V_s$ . As  $V_s \rightarrow 0$ , clearly  $\mu_{ij}$  also vanishes since there are no longer any trapped particles, see Fig. 7. However, as  $V_s/T_b \rightarrow \infty$ , Eqs. (259) and (261) imply that  $\mu_{11} \rightarrow \infty$  as well, roughly as  $\exp(V_s/T_b)$ . The reason for this divergence is that particles trapped by the squeeze take arbitrarily large steps as  $\omega_0 \rightarrow 0$  [see Eq. (252)], unless their drift step is interrupted by collisional detrapping. For  $\omega_0 \rightarrow 0$ , the field error allows trapped particles to drift all the way to the wall. The probability of becoming detrapped scales as  $\exp(-V_s/T_b)$  for large  $V_s/T_b$ , so the size of the drift step scales as the inverse of this factor. Of course, this estimate neglects variation in  $\omega_0$  as a function of  $r$ , since as particles drift to large  $r$  the rotation frequency can change so that  $\omega_0$  is no longer much smaller than  $\nu$ . However, this effect is beyond the local approximation, and is not included here.

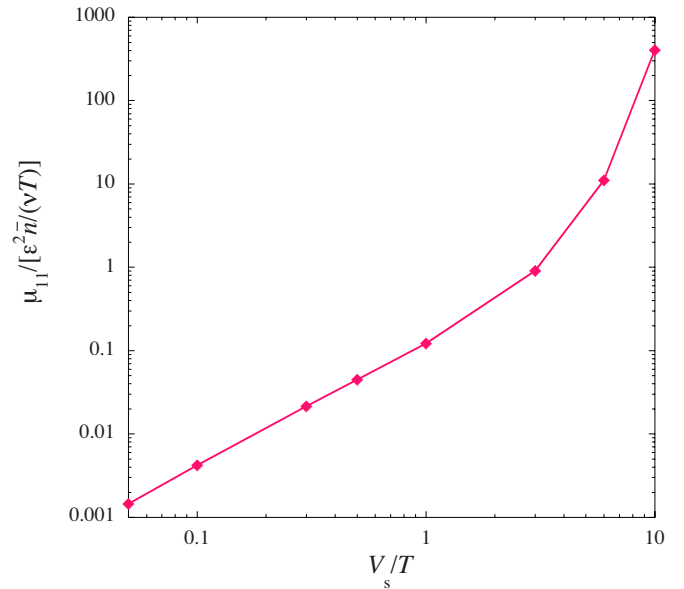


FIG. 7. (Color online)  $\mu_{11}$  vs squeeze potential  $V_s$  in the  $1/\nu$  regime, for the model of example 3.

The coefficient  $\mu_{33}$  is not divergent as  $V_s/T_b \rightarrow \infty$ , and  $\mu_{31}$  diverges only linearly with  $V_s/T_b$ . This is because, although radial drift steps are becoming large for large  $V_s/T_b$ , the particle energies are still thermalized on a time scale set by  $\nu$ , so the effective radial energy step remains finite.

Note that if  $\omega_0 \rightarrow 0$ , the  $1/\nu$  transport scaling leads to very large transport for small  $\nu/k\bar{v}$ , as shown in Fig. 5. This could be observed in experiments where the field error rotates with the plasma. Thus, adding a squeeze potential could increase the coupling efficiency of rotating field errors that are used to provide steady-state plasma confinement.<sup>33</sup>

## 2. $\nu < \omega_0 < k\bar{v}$ : The $\sqrt{\nu}$ regime

As  $\nu$  decreases below  $\omega_0$ , particles are able to execute entire  $\mathbf{E} \times \mathbf{B}$  drift orbits in the  $r-\theta$  plane so that the maximum drift-step size of  $\Delta r$  is achieved, where  $\Delta r$  is given by Eq. (252). The diffusion due to these steps scales as  $\nu(\Delta r)^2$ ; it decreases linearly as  $\nu$  decreases. However, in this regime a new effect supercedes this result. Trapped particles execute a different drift orbit than untrapped particles, leading, in the absence of collisions, to a discontinuity in the perturbed distribution function at the separatrix between trapped and untrapped particles. However, collisions smooth out the discontinuity over a boundary layer with width of order  $\sqrt{\nu/\omega_0} T_b$  in energy. The dissipation of energy created by this boundary layer leads to transport that scales as  $\sqrt{\nu/\omega_0}$ , which dominates at small  $\nu$ .<sup>25,26</sup>

The magnitude of this effect can still be determined using the bounce-averaged equations for the trapped particle distribution, Eq. (253). When  $\nu/\omega_0$  is small, the equation may be solved using a boundary layer analysis. We replace  $I(E)$  by its value on the separatrix,  $I_s \equiv I(V_s)$ . The function  $\tau(E) = \partial I / \partial E$  has logarithmic divergence over an exponentially narrow range of energies near the separatrix. Here we assume that  $\sqrt{\nu/\omega_0}$  is small, but is still large compared to the

width of this divergence, and we replace  $\tau(E)$  by the average value of  $\tau(E)$  averaged over the energy range  $\sqrt{\nu/\omega_0}T_b$  near the separatrix,

$$\tau_s = \frac{\sqrt{\omega_0/\nu}}{T_b} \int_{V_s - \sqrt{\nu/\omega_0}T_b}^{V_s} \tau(E) dE. \quad (265)$$

Also, we note that the second-derivative term in Eq. (256) dominates in the boundary layer, so we replace Eq. (256) by

$$-i\ell\omega_0\tau_s\bar{g}_{j\ell} - \nu T_b I_s \frac{\partial^2 \bar{g}_{j\ell}}{\partial E^2} = \tau_s \bar{s}_{j\ell}. \quad (266)$$

The solution to Eq. (266) that matches the boundary condition that  $\bar{g}_{j\ell}(V_s)=0$ , and which decreases as  $E$  decreases, is

$$\bar{g}_{j\ell} = i \frac{\bar{s}_{j\ell}(V_s)}{\ell\omega_0} \left\{ 1 - e^{-[1-i \operatorname{sgn}(\ell\omega_0)]/\sqrt{2}(V_s-E)\sqrt{|\ell\omega_0|\tau_s/\nu I_s T_b}} \right\}. \quad (267)$$

Applying this result to the calculation of  $\mu_{ij}$  via Eq. (259), noting again that  $\bar{g}_{j\ell}(E)$  is nonzero only within the boundary layer so that we may replace  $\tau(E)$  by  $\tau_s$  and  $\bar{s}_{j\ell}(E)$  by  $\bar{s}_{j\ell}(V_s)$ , we then perform the energy integration to obtain

$$\begin{aligned} \mu_{ij} &= \frac{2\bar{n}}{T_b} \int_{-\infty}^{\infty} dz e^{-\phi_0/T} \sqrt{\frac{2\pi}{mT_b}} e^{-V_s/T_b} \tau_s \sum_{\ell} \frac{\bar{s}_{j\ell}(V_s) \bar{s}_{i\ell}^*(V_s)}{|\ell\omega_0|} \\ &\times \frac{1}{4} \sqrt{\frac{2\nu I_s T_b}{|\ell\omega_0|\tau_s}}, \end{aligned} \quad (268)$$

valid for  $\nu/\omega_0 \ll 1$  and  $\omega_0/k\bar{v} \ll 1$ .

Also, this result requires that the width of the collisional boundary layer at the separatrix be small compared to  $V_s$ ,

$$\sqrt{\frac{2\nu I_s T_b}{|\ell\omega_0|\tau_s}} \ll V_s. \quad (269)$$

For a long plasma of length  $L$  with flat ends,  $I_s \approx L\sqrt{2mV_s}/\pi$  and  $\tau_s \approx L/\pi\sqrt{2V_s/m}$ , this inequality can be written as

$$\frac{4\nu}{|\ell\omega_0|} \ll \frac{V_s}{T_b}. \quad (270)$$

A simplified version of Eq. (268) can be obtained by using these forms for  $\tau_s$  and  $I_s$ , and substituting  $L$  for  $\int_{-\infty}^{\infty} dz e^{-\phi_0/T_b}$ . The result for  $\mu_{ij}$  in the  $\sqrt{\nu}$  regime for a long plasma column with flat ends is

$$\mu_{ij} \approx \frac{1}{\sqrt{\pi}} \sum_{\ell} \frac{\bar{n}}{|\ell\omega_0|T_b} \sqrt{\frac{\nu}{|\ell\omega_0|}} e^{-V_s/T_b} \bar{s}_{j\ell}(V_s) \bar{s}_{i\ell}^*(V_s). \quad (271)$$

This is independent of plasma length  $L$  and, for  $V_s/T_b \rightarrow 0$ , is nonzero [note that Eq. (270) must be satisfied, however]. Thus, even a weak squeeze potential can have a strong effect on the transport in the  $\sqrt{\nu}$  regime. This is because the transport depends only on the particles in the thin boundary layer, whose properties are independent of  $V_s$  if  $V_s \ll T_b$  and Eq. (270) is satisfied.

Equation (268) is compared to simulations of particle diffusion in Fig. 5 at two different rotation frequencies.

When  $\nu/\omega_0$  is sufficiently small, the theory matches the simulation results well. Also, by comparing Figs. 5 and 3(a), we can see that the  $\omega_0/k\bar{v}=0.1$  data exhibits a decrease in  $\mu_{11}$  compared to the case where no squeeze potential is applied. Only for  $\omega_0/k\bar{v} \ll 1$  does the applied squeeze enhance the transport above the level where no squeeze is applied.

## V. DISCUSSION

In this paper we have presented a general theory of magnetized plasma transport driven by electrostatic field asymmetries. A local approximation to the kinetic equation, valid in the transport limit where the field error potential is much smaller than the plasma temperature, allows the determination of local transport coefficients that link dissipative cross-field particle, momentum and energy fluxes to plasma rotation, parallel velocity, and temperature and velocity gradients. In particular, temperature-gradient-driven particle flux can be important if the gradient is sufficiently large. In non-neutral plasma experiments such large temperature gradients often develop naturally during the transport process itself, as the plasma expands radially and converts some of its electrostatic potential energy into heat. The self-consistent evolution of temperature and density profiles under the action of static field errors will be considered in later work.

For plasmas with axial symmetry at zeroth order (i.e., neglecting the field errors), axial forces develop due to plasma rotation and temperature gradients in the presence of the field errors. Such forces could play a role in determining the toroidal rotation observed in some experiments.<sup>34–36</sup>

Three examples of field error transport were considered, and particle simulations were used to test the theory. In each case, the transport simulations agreed with the theory. However, detailed comparisons of the type done here require rather precise knowledge of the plasma potential, both of the zeroth-order equilibrium and the asymmetry. For instance, in the plateau regime of examples 1 and 2, the transport coefficients were observed to depend sensitively on both the plasma rotation frequency and on the presence or absence of an axial trapping field. Also, it was observed that if, in the zeroth order equilibrium, there exists separate trapped particle populations caused by an azimuthally symmetric squeeze potential, and if the rotation frequency is small compared to the bounce frequency, the transport is strongly modified from the banana and plateau regime predictions. New  $1/\nu$  and  $\sqrt{\nu}$  regimes were found similar to those predicted in neoclassical transport theory for toroidal plasmas. Even a small population of such trapped particles completely changed the magnitude and scaling of the transport from theory predictions in the absence of trapping.

The challenge to experimentalists will be to characterize the plasma potential with sufficient accuracy so as to make contact with these theory results. A detailed comparison of experiment with theory will be left to a future paper, but suffice to say that current experimental results are still apparently in disagreement with the theory presented here. In particular, radial particle transport for experiments with an equilibrium squeeze, carried out in the  $\sqrt{\nu}$  regime, do not have the same magnetic field scaling as the theory. In general, our

theory predicts that the magnetic field enters the radial particle mobility coefficient in only two ways: through an overall multiplicative factor (of  $1/B^2$ ), and through the plasma rotation frequency. (The same may be said for the plasma density.) In the  $\sqrt{\nu}$  regime this leads to a prediction of radial mobility scaling as  $1/\sqrt{B}$ , but a stronger dependence on  $1/B$  is observed in experiments.<sup>20</sup>

One possible explanation for this anomaly is that the field errors used in the theory examples are missing some essential component. Another possibility is that a magnetic nonuniformity, neglected in the theory presented here, is responsible for the transport. A third possibility is that the collective response of the plasma to the field error is important, such as the presence of a low-frequency plasma mode that is driven by the error. And of course, the final possibility is that some unknown effect is causing the transport. It is hoped that, through detailed theory and experiment comparisons, we will eventually be able to arrive at a theory that explains the experiments. In the meantime, such studies will certainly continue to shed much-needed light on the richly varied behavior of plasmas interacting with field asymmetries.

## ACKNOWLEDGMENTS

The author is indebted to Professor C. F. Driscoll for many useful conversations.

This work was supported by National Science Foundation Grant No. PHY-0354949 and NSF/DOE Grant No. PHY-0613740.

## APPENDIX A: VARIATIONAL PRINCIPLE

The local entropy production rate, Eq. (110), can be used as the basis for a variational principle from which the transport coefficients can be derived without having to directly solve the kinetic equation.<sup>1,24,30</sup> The principle is written in terms of distribution functions  $g^+$  and  $g^-$  that are even and odd respectively under time reversal,

$$\begin{aligned} g^+ &= (g + g^\dagger)/2, \\ g^- &= (g - g^\dagger)/2. \end{aligned} \quad (\text{A1})$$

Then  $g = g^+ + g^-$  and we can write  $\dot{S}$  as

$$\dot{S} = -(g^+, \hat{C}g^+)_{p_\theta} - (g^-, \hat{C}g^-)_{p_\theta} - 2(g^+, \hat{C}g^-)_{p_\theta}, \quad (\text{A2})$$

where in the last term we have used the Hermitian property of  $\hat{C}$ .

Equations of motion for  $g^+$  and  $g^-$  follow by adding and subtracting Eq. (69) from its time-reversed version. Here we assume for simplicity that we are dealing with a portion of  $s$  which is even under time-reversal, and also assume a non-conservative collision operator so that only  $\lambda_1 \neq 0$  is required. Then the equations for  $g^+$  and  $g^-$  are

$$\hat{A}g^- - \hat{C}g^+ = s - \lambda_1^+, \quad (\text{A3})$$

$$\hat{A}g^+ - \hat{C}g^- = -\lambda_1^-, \quad (\text{A4})$$

where  $\lambda_1^+ = (\lambda_1 + \lambda_1^\dagger)/2$  and  $\lambda_1^- = (\lambda_1 - \lambda_1^\dagger)/2$ , with these constants determined by the constraints that

$$(g^+, 1)_{p_\theta} = (g^-, 1)_{p_\theta} = 0. \quad (\text{A5})$$

Now consider the following functional of  $g^+$  and  $g^-$ ,

$$\begin{aligned} F &= -(g^+, \hat{C}g^+)_{p_\theta} - (g^-, \hat{C}g^-)_{p_\theta} - 2(g^+, \hat{A}g^- - \hat{C}g^+ - s)_{p_\theta} \\ &\quad - 2\lambda_1^+(g^+, 1)_{p_\theta} + 2\lambda_1^-(g^-, 1)_{p_\theta}. \end{aligned} \quad (\text{A6})$$

Variation of this functional with respect to  $g^+$  and  $g^-$  yields Eqs. (A3) and (A4). Note that here  $\lambda_1^+$  and  $\lambda_1^-$  enter as Lagrange multipliers used to satisfy constraints (A5).

Also, at the extremum,  $F = \dot{S}$ . This follows because at the extremum equations (A3)–(A5) imply that all but the first two inner products in  $F$  vanish, and in Eq. (A2) the last inner product vanishes since Eq. (A4) implies that

$$(g^+, \hat{C}g^-)_{p_\theta} = (g^+, \hat{A}g^+)_{p_\theta} + \lambda_1^-(g^+, 1)_{p_\theta} = 0 \quad (\text{A7})$$

(recall that  $\hat{A}$  is anti-Hermitian). Thus, extremizing  $F$  yields  $\dot{S}$ , which is directly related to the transport coefficients through Eq. (113).

Furthermore, by taking a second variation of  $F$  it is easily seen that  $F$  is maximized under variation of  $g^+$ , and minimized under variation of  $g^-$ . However, in numerical work it is more convenient to deal with a pure maximum or minimum, rather than a saddle. This can be accomplished by using Eq. (A4) in Eq. (A6), which allows us to write  $F$  as

$$F = (g^+, \hat{C}g^+)_{p_\theta} + (g^-, \hat{C}g^-)_{p_\theta} + 2(g^+, s)_{p_\theta} - 2\lambda_1^+(g^+, 1)_{p_\theta}. \quad (\text{A8})$$

Since we must now consider  $g^-$  to be determined as a functional of  $g^+$  through the solution of Eq. (A4), then  $F$  is clearly maximized with respect to variations of  $g^+$ . Furthermore, it is not difficult to solve Eq. (A4) for  $g^-$ , by expanding  $g^-$  in the eigenfunctions  $H_n$  of  $\hat{C}$ ,

$$\hat{C}H_n = -\nu_n H_n, \quad (\text{A9})$$

where  $\nu_n = n\nu$  for the collision operator of Eq. (117), and  $H_0 = 1$ . The solution is

$$g^- = \sum_{n=1}^{\infty} g_n^- H_n + g_0^-(p_\theta, \theta, z), \quad (\text{A10})$$

where

$$g_n^- = -(H_n, \hat{A}g^+)_{p_z} / \nu_n (H_n, H_n)_{p_z}, \quad (\text{A11})$$

and  $g_0^-$  is an undetermined function. Here,  $(g, h)_{p_z} \equiv \int dp_z f_0 g h$ , and the eigenfunctions  $H_n$  are assumed to be orthogonal with respect to this inner product. If we also write  $g^+$  as a sum of eigenfunctions,

$$g^+ = \sum_{n=0}^{\infty} g_n^+ H_n, \quad (\text{A12})$$

and substitute these expressions into Eq. (A8), we obtain

$$F = - \sum_{n=1}^{\infty} \nu_n [(g_n^+ H_n, g_n^+ H_n)_{p_\theta} + (g_n^- H_n, g_n^- H_n)_{p_\theta}] + 2 \sum_{n=0}^{\infty} (g_n^+ H_n, s)_{p_\theta} - 2\lambda_1^+(g_0^+, 1)_{p_\theta}, \quad (\text{A13})$$

with  $g_n^-$  given by Eq. (A11). Note that the last term in  $F$  can be dropped provided that a representation of  $g_0^+$  is employed (for example, through an expansion in basis functions) for which  $(g_0^+, 1)_{p_\theta} = 0$ . Maximization of  $F$  with respect to the set of functions  $g_n^+(p_\theta, \theta, z)$  yields the entropy production rate  $\dot{S}$ , and hence the transport coefficients via Eq. (113), without having to directly solve the kinetic equation.

## APPENDIX B: FLUID REGIME RESULTS FOR A CONSERVATIVE COLLISION OPERATOR

In this appendix we derive transport coefficients in the fluid regime  $\nu \gg k\bar{v}$  for the Hamiltonian of example 1, using a collision operator that conserves energy and momentum as well as particle number. We employ a version of the Dougherty collision operator<sup>31</sup> that involves only parallel momentum:

$$\hat{C}f = D \frac{\partial}{\partial p_z} \left[ \frac{\partial f}{\partial p_z} + \frac{p_z - mV(f)}{mT(f)} f \right], \quad (\text{B1})$$

where the fluid velocity  $V$  and temperature  $T$  are

$$V(f) = \int dp_z f p_z / \int dp_z m f, \quad (\text{B2})$$

and

$$T(f) = \int dp_z f (p_z - mV)^2 / \int dp_z m f. \quad (\text{B3})$$

Then the operator  $\hat{C}$  corresponding to  $\hat{C}$  [see Eq. (48)] is

$$\hat{C}g = D \left( \frac{\partial^2 g}{\partial p_z^2} - \frac{p_z'}{T_0} \frac{\partial g}{\partial p_z} \right) + \nu \left[ \frac{\Delta V p_z'}{T_0} + \frac{\Delta T}{T_0} \left( \frac{p_z'^2}{mT_0} - 1 \right) \right], \quad (\text{B4})$$

where we have linearized in  $\delta\phi$ , and where

$$\Delta V = \frac{\int f_{00} g p_z' dp_z}{m \int f_{00} dp_z} \quad (\text{B5})$$

and

$$\Delta T = \frac{\int f_{00} g (p_z'^2/m - T_0) dp_z}{\int f_{00} dp_z} \quad (\text{B6})$$

are the velocity and temperature perturbation associated with  $g$ ,  $p_z' = p_z - m\bar{V}$ , and  $\bar{V} = V(f_{00})$  is the equilibrium velocity. The eigenfunctions of  $\hat{C}$  are still the Hermite polynomials  $H_n(p_z'/\sqrt{2mT_0})$ , and for  $n \geq 3$  the eigenvalues are unchanged,

$$\hat{C}H_n = -n\nu H_n, \quad n \geq 3. \quad (\text{B7})$$

However, for  $n=0, 1$ , and  $2$ , the eigenvalues are now zero, as expected for conservative collisions. Equations (166) and (167) are then replaced by

$$2\sqrt{2}k\bar{v}\tilde{g}_2 - \ell\omega_0'\tilde{g}_1 + \frac{k\bar{v}}{\sqrt{2}}\tilde{g}_0 = \frac{\ell\varepsilon}{2} \left\{ 0, \frac{m\bar{v}}{\sqrt{2}}, 0 \right\}, \quad (\text{B8})$$

$$3\sqrt{2}k\bar{v}\tilde{g}_3 - \ell\omega_0'\tilde{g}_2 + \frac{k\bar{v}}{\sqrt{2}}\tilde{g}_1 = \frac{\ell\varepsilon}{2} \{0, 0, 1/4\}.$$

All other equations for  $\tilde{g}_n$  remain the same (with the substitution  $\omega_0'' \rightarrow \omega_0' \equiv \omega_0 - k_z \bar{V} / \ell$ ).

Since the first three equations in the sequence, Eqs. (165) and (B8), no longer depend on collision frequency, the next equation involving  $\tilde{g}_4$  must also be kept in order to obtain nontrivial results for the transport coefficients. To lowest order in  $1/\nu$ , one can set  $\tilde{g}_4 = 0$  and solve the four equations for  $(\tilde{g}_0, \tilde{g}_1, \tilde{g}_2, \tilde{g}_3)$ . This results in a matrix of transport coefficients with the same form as Eq. (161) (except that  $\omega_0'' \rightarrow \omega_0'$ ), but now

$$\mu_{11} = \frac{\ell^2 \varepsilon^2 \bar{n}}{T_0} \frac{k^6 \bar{v}^6 \nu}{\ell^2 \nu^2 \omega_0'^2 (3k^2 \bar{v}^2 - \ell^2 \omega_0'^2)^2 + F \left( \frac{\ell \omega_0'}{k\bar{v}} \right) k^8 \bar{v}^8}, \quad (\text{B9})$$

$$\mu_{13} = \frac{\ell^2 \varepsilon^2 \bar{n}}{2T_0} \frac{k^4 \bar{v}^4 \nu (\ell^2 \omega_0'^2 - k^2 \bar{v}^2)}{\ell^2 \nu^2 \omega_0'^2 (3k^2 \bar{v}^2 - \ell^2 \omega_0'^2)^2 + F \left( \frac{\ell \omega_0'}{k\bar{v}} \right) k^8 \bar{v}^8}, \quad (\text{B10})$$

and

$$\mu_{33} = \frac{\ell^2 \varepsilon^2 \bar{n}}{4T_0} \frac{k^2 \bar{v}^2 \nu (\ell^2 \omega_0'^2 - k^2 \bar{v}^2)^2}{\ell^2 \nu^2 \omega_0'^2 (3k^2 \bar{v}^2 - \ell^2 \omega_0'^2)^2 + F \left( \frac{\ell \omega_0'}{k\bar{v}} \right) k^8 \bar{v}^8}, \quad (\text{B11})$$

where the function  $F(x)$  is needed only near  $x=0$  and  $x = \pm\sqrt{3}$ , since only for these values of the argument is the term involving  $F$  important. For these values, it may be shown that

$$F(0) = 1 \quad \text{and} \quad F(\pm\sqrt{3}) = 4. \quad (\text{B12})$$

<sup>1</sup>F. L. Hinton and R. D. Hazeltine, *Rev. Mod. Phys.* **48**, 239 (1976).

<sup>2</sup>H. E. Mynick, *Phys. Plasmas* **13**, 058102 (2006).

<sup>3</sup>F. L. Hinton and M. N. Rosenbluth, *Phys. Fluids* **16**, 836 (1983).

<sup>4</sup>R. D. Hazeltine, F. L. Hinton, and M. N. Rosenbluth, *Phys. Fluids* **16**, 1645 (1973).

<sup>5</sup>Z. Parsa, S. Tepikian, and E. Courant, *Part. Accel.* **22**, 205 (1987).

<sup>6</sup>B. E. Carlsten, *Proceedings of the 1987 IEEE Particle Accelerator Conference* (IEEE, New York, 1987), p. 1755.

<sup>7</sup>S. Fujimura, A. Ueno, and Y. Yamazaki, *Proceedings of the 10th Symposium on Accelerator Science and Technology* (JAERI, Japan, 1995), p. 254.

<sup>8</sup>N. J. Fisch, *Rev. Mod. Phys.* **59**, 175 (1987).

- <sup>9</sup>N. J. Fisch, *Plasma Phys. Controlled Fusion* **35**, A91 (1993).
- <sup>10</sup>M. Porkolab, *Theory of Magnetically Confined Plasmas* (Pergamon, Oxford, 1976), p. 339.
- <sup>11</sup>T. H. Stix, *Symposium on Plasma Heating and Injection* (Editrice Compositori, Bologna, Italy, 1973), p. 8.
- <sup>12</sup>F. Chen, *Introduction to Plasma Physics* (Plenum, New York, 1974), p. 229.
- <sup>13</sup>V. E. Zakharov and V. I. Karpman, *Sov. Phys. JETP* **16**, 351 (1963).
- <sup>14</sup>J. H. Malmberg and C. B. Wharton, *Phys. Rev. Lett.* **13**, 184 (1964).
- <sup>15</sup>J. R. Danielson, F. Anderegg, and C. F. Driscoll, *Phys. Rev. Lett.* **92**, 245003 (2004).
- <sup>16</sup>T. Ohkawa, J. R. Gilleland, and T. Tamano, *Phys. Rev. Lett.* **28**, 1107 (1972).
- <sup>17</sup>J. H. Malmberg and C. F. Driscoll, *Phys. Rev. Lett.* **44**, 654 (1980).
- <sup>18</sup>C. F. Driscoll and J. H. Malmberg, *Phys. Rev. Lett.* **50**, 167 (1983).
- <sup>19</sup>D. L. Eggleston and B. Carillo, *Phys. Plasmas* **10**, 1308 (2003).
- <sup>20</sup>A. A. Kabantsev, J. H. Yu, R. B. Lynch, and C. F. Driscoll, *Phys. Plasmas* **10**, 1628 (2003).
- <sup>21</sup>F. L. Hinton and S. K. Wong, *Phys. Fluids* **28**, 3082 (1985).
- <sup>22</sup>R. H. Cohen, *Nucl. Fusion* **19**, 1579 (1979).
- <sup>23</sup>A. A. Galeev and R. Z. Sagdeev, *Sov. Phys. JETP* **26**, 233 (1968).
- <sup>24</sup>M. N. Rosenbluth, R. D. Hazeltine, and F. L. Hinton, *Phys. Fluids* **15**, 116 (1972).
- <sup>25</sup>M. N. Rosenbluth, D. W. Ross, and D. P. Kostomarov, *Nucl. Fusion* **12**, 3 (1972).
- <sup>26</sup>T. J. Hillsabeck and T. M. O'Neil, *Phys. Plasmas* **10**, 3492 (2003).
- <sup>27</sup>G. B. Arfken and H. J. Weber, *Mathematical Methods for Physicists* (Academic, New York, 2005).
- <sup>28</sup>In the banana regime this modification shifts the trapping frequency. For the Hamiltonian of Example 1, the shift is negligible provided that  $|\partial\omega_0/\partial p_\theta| \ll k^2/m^2$ . This ordering is assumed in the local approximation. See D. L. Eggleston and T. M. O'Neil, *Phys. Plasmas* **6**, 2699 (1999).
- <sup>29</sup>L. E. Reichl, *A Modern Course in Statistical Physics* (University of Texas Press, Austin, 1980).
- <sup>30</sup>F. L. Hinton and M. N. Rosenbluth, "Variational principle for neoclassical transport properties," Trieste: International Atomic Energy Agency and United Nations Educational Scientific and Cultural Organization Informal Report No. IC/70/111 (1970).
- <sup>31</sup>J. P. Dougherty, *Phys. Fluids* **7**, 1788 (1964).
- <sup>32</sup>A. Gibson and D. W. Mason, *Plasma Phys.* **11**, 121 (1969).
- <sup>33</sup>X.-P. Huang, F. Anderegg, E. M. Hollmann, C. F. Driscoll, and T. M. O'Neil, *Phys. Rev. Lett.* **78**, 875 (1977).
- <sup>34</sup>M. G. Bell, *Nucl. Fusion* **19**, 33 (1979).
- <sup>35</sup>J. E. Rice, E. S. Marmor, F. Bombarda, and L. Qu, *Nucl. Fusion* **37**, 421 (1997).
- <sup>36</sup>W. M. Stacey, *Phys. Plasmas* **11**, 3096 (2004).